

# Stronger Educational Performance in Early Life Correlates with Higher Cancer Risk, Lower Dementia Risk and Lower All-cause Mortality in Later Life – but Why?

Anatoly Mayburd (✉ [mail@inventomika.org](mailto:mail@inventomika.org))

George Mason University

---

## Research Article

**Keywords:** nervous system, organs, oncogenesis, hypothesis , academic performance

**Posted Date:** April 28th, 2021

**DOI:** <https://doi.org/10.21203/rs.3.rs-460229/v1>

**License:** © ⓘ This work is licensed under a Creative Commons Attribution 4.0 International License. [Read Full License](#)

---

## Abstract

Better functioning nervous system stimulates other organs, promoting longevity. As a trade-off, this stimulation may result in enhanced oncogenesis.

This hypothesis was tested by analyzing factors reflecting cognitive score and academic performance. Educational performance emerged as a universal independent negative correlate for most of comorbidities, except cancer, that forms a positive correlate. More educated individuals demonstrate more aggressive neoplasia and cancer patients demonstrate lesser mental and physical decline as compared with controls. Cognitive stability and high cognitive score were the statistically strongest anti-correlates of all-cause mortality, pointing to neurological health as the principal mediator of survival.

The patients remaining clinically normal despite decreased cognitive scores demonstrated anomalously low mortality (~2.5% annual in the 90 years old). Such “dementia resister” phenotype was more prevalent in the higher education cohorts, which also demonstrated a delayed aging rate. Remaining life expectancy was linearly proportional to the baseline cognitive score.

We proposed that systemic non-trauma mobilization of stem-cell activity by CNS acts as a permanent regenerative endogenous factor with the trade-off of increased cancer risk due to similar interactions with cancer stem cells. Novel markers of mortality risk can follow as practical applications.

## Introduction

A fascinating link of brain and longevity is known since the 19-th century [Beard et al.]. At least in mammals and birds, maximal total and reproductive lifespan correlates with brain size [Minias et al., Rushton et al., Peters et al.]. In humans, longevity was found to correlate not only with brain size but with the observed IQ [Rushton et al.]. Human brain was found to consume up to 20% of the total body energy supply, while in shorter living animals such as rats, cats, and dogs this percentage is 4–6%. [Peters et al.]. Compared to shorter-living ape species, humans display faster metabolism, and theoretically should also age faster – but instead demonstrate higher fecundity and greater lifespan [Pontzer et al.]. Not only brain size, but its qualitative characteristics serve as lifespan correlates [Gottfredson et al., Deary et al.]. According to Gottfredson et al., the role of intelligence in longevity is to mainly improve adaptation to the environment, maintain healthy lifestyle and avoid danger [Gottfredson et al.]. However, this is a limited view. Intelligence can predict mortality irrespective to the environmental context and more strongly than body mass index, total cholesterol, blood pressure or blood glucose, and at a similar level to smoking [Deary et al.]. Deary et al. reports that higher intelligence test scores were associated with a lower probability of developing metabolic syndrome in middle age. The individuals more dependable or conscientious in childhood and scoring in the top 50% of the population for intellect and dependability were twice as likely to survive past 60 as compared to the bottom of the rank [Deary, Batty et al.].

In one scenario, a signal pathway in neurons involves receptors coupled to phosphatidylinositol-3-kinase, Akt and glycogen synthase kinase-3 $\beta$  may regulate longevity via the brain [Mattson et al.]. Central nerve system BDNF signaling can increase peripheral insulin sensitivity and indeed endocrine health is worse in the students with mental retardation [Pandit et al.]. NAD<sup>+</sup> availability decreases with age, reducing sirtuin activities, altering communication between the hypothalamus and adipose tissue at a systemic level. These processes likely contribute to the development of diseases of aging [Imai et al.]. Still other criteria in brain-mediated longevity reside in the state of glia. Unfolded proteins normally trigger the unfolded protein response (UPR), and neurons communicate activation of the UPR to peripheral tissues to promote longevity in the nematode *Caenorhabditis elegans*. Glial cells can also initiate long-range activation of the endoplasmic reticulum UPR (UPRER) in distal cells orchestrating stress resistance and promoting longevity in *C. elegans* via neuropeptide secretion [Miklas et al.]. The glial longevity control is effective in mammals too. Selective elimination of senescent glia cells led to reversal of cognitive decline in a murine model [Bussian et al.], and anti-senescence treatments are at the forefront of healthy longevity effort. Transplanting relatively small numbers of senescent cells into young mice is sufficient to spread cellular senescence to the recipient tissues and cause functional deterioration. Transplanting even fewer senescent cells had the same effect in older recipients and was accompanied by reduced survival [Xu et al.].

Finally, the diverse signaling of hypothalamic and peripheral stem cells niches may impact lifespan. Intravenous injection of umbilical cord-derived mesenchymal stem cell in the human patients with vascular dementia increased MMSE score from ~ 15 to ~ 19 within 3 months, but the scores reverted to ~ 14 within 6 months, demonstrating a causative link between the presence of circulating stem cells and cognitive status [He et al.]. Cognitive status in turn correlates with survival [Cole et al.].

Perhaps all or some components in the brain/longevity axis described above contribute to the outcomes with varying weights. Yet there is a need to present a hypothesis that explains as wide a range of facts as possible. Such a concept can guide future effort in minimization of chronic disease, extending healthy lifespan and cutting premature mortality in surgeries, traumas, and infections. The components not

considered previously, while analyzing brain/longevity relationship are the interactions between nervous system and tumorigenicity, as well as between cancer and dementia.

The connection between oncogenesis and neurogenesis is fascinating. Autonomic nerve fibres in the tumor microenvironment regulate cancer initiation and dissemination, and stimulating peripheral nerves emerge in tumors. Circulating neural progenitors exiting directly from the central nervous system infiltrate tumors and metastases, in which they initiate neurogenesis and increase the level of aggressiveness [Tara et al., Mauffrey P et al; Dart et al]. The overlap of molecular pathways involved in cancer and Alzheimer's disease are reviewed in [Nudelman et al.], and competing epidemiological relationship is mentioned in extensive literature exemplified by [Shafi et al; Zhang et al; van der Willik et al.].

In this report we present additional data, which, together with the presented context support a new hypothesis linking brain activity and lifespan. We propose the role of nerve system in activation and mobilization of stem cells permeating to a various degree all organ systems. The concept explains a broad range of phenomena reported in the literature, combining 9 independent datasets and  $> 10^6$  respondents.

## Results

### Factor analysis of chronic disease and mortality in NBER, NHIS, NSHAP, TILDA, MIDUS, CLHLS and Kaiser Permanente Study of the Oldest Old.

Figure 1A presents the summary data for the 606228 cancer patient decedents (neoplasia as the primary diagnosis) and 1604462 non-cancer/non-dementia controls. The data were collected for the years 1999, 2004, 2011 and 2017 in the National Bureau of Economic Research (NBER) depository [NBER]. The results show a consistent trend of greater educational attainment in the cancer decedents vs. the same in the control, exceeding the margin of random error (CI95). The individuals with the shorter lifespans (plotted on the abscissa) demonstrate greater absolute and relative differences in educational performance, with the cancer patients outperforming. The extent of the outperforming is attenuated for the longer lifespans.

Figure 1B presents the correlation of the life-long educational attainment with the number of cancer foci in the individuals. To ensure that the age differences between these subsets do not introduce a biasing trend, the ages of the groups were equalized at 78 ( $\pm 0.5$ ) years each. Under these conditions, a monotonous increase in lifelong educational performance becomes a correlate of cancer spread (*foci* number in different tissues).

Figure 1C explores reproducibility of the relationship between education and cancer in additional datasets [Wisconsin Longitudinal Study, TILDA, NHIS], composed of living individuals and measuring cancer prevalence (not mortality). In all of them (W, T and N), the increase in educational achievement parallels decreased all-cause mortality rate, increased cancer prevalence rate and decreased multimorbidity (cardiovascular, stroke, diabetes, renal and pulmonary). The odds ratio of cancer to serious non-cancer comorbidity varies  $\sim 2$ -fold between the most and least educated population strata across these 3 datasets. The individuals with higher education demonstrate lower rate of physical disability and polypharmacy, higher self-assessed health, visual acuity, and cognitive performance and are taller than the less educated counterparts. They also demonstrate lower smoking rate (but higher cancer rate despite lower smoking rate). Our results confirm that educational performance is an important health and longevity predictor [Gotfredson et al., Deary et al] (Figure 1A-C).

The cancer-education relationship extracted in NBER reproduces in similar formats in National Social Life, Health, and Aging Project (NSHAP) 2005-2011 [NSHAP] and in National Health Interview Survey (NHIS) 1994-2000 [NHIS]; with the results presented in Figure 2A-C.

Figure 2A presents the data of NHIS survey showing the consistently increased educational performance for the cancer patients vs. the non-dementia control [Sun et al.; Hayes-Larson et al.]. Figure 2B presents the data for the NSHAP survey showing a significantly higher cognitive score in neoplasia and a slower rate of cognitive decline vs. control, especially in more advanced ages. Figure 2C presents the positive correlation of the education level in the NSHAP individuals with the variable number of neoplasia foci.

A review of additional datasets identified a further list of behavioral factors correlating with the cancer prevalence (Supplemental Table 1). The analysis includes Midlife in the United States (MIDUS) series [MIDUS], the National Health Interview Survey (NHIS) series [NHIS] and the Social Life, Health and Aging Project (NSHAP) [NSHAP].

Supplemental Table 1 presents cancer and control cohorts carefully balanced by age, gender, race, and non-cancer comorbidity in the NBER, MIDUS, NHIS and NSHAP sources. The presence of neoplasia and its correlates differentiates the cohorts, explaining the higher mortality rates, lower lifespans, and lower self-assessed physical health in the cancer cohort. Despite lower vitality in the neoplasia cohorts, the cohort members display statistically significant higher educational achievement (A1PB1, SF53, EDUC), a trend to greater personal independence

(A1SF1Z, SF3448, SF491), a stronger sense of duty (A1SK7K, SF507), a trend to maintain relationships (SF48, MARITLST), higher household income (A1PC8, A1SJ13, SF58, SF61, SF3448, SF3548, [Larsen et al.]), altruistic behaviors (A1SK6F, SF533), higher cognitive ability (MOCA score).

Physical features are also contributing to the distinction between the cohorts, such as height (A1SA25, SF93), waist-to-hip ratio (A1SWSTHI), BMI (A1SBMI), (WAIST x HIP)/HEIGHT<sup>2</sup>, systolic blood pressure (SYSTOLIC\_1, 2), changes in sexuality (SEXCHGES). A consistent biological distinction is the smaller size of household in the present and future neoplasia patients (A1PB35, A1SE18B, SF2051) and the gender of the first child (A1PB36A1). The emotional abuse in childhood (A1SE17E), smoking and greater alcohol use in the cancer patients suggest both higher stress level in the neoplasia cohort [Kruk et al.] and direct carcinogenic effect of alcohol and tobacco [Klein et al.]. Higher arthritis incidence in cancer as well as higher supplement use in neoplasia suggests more advanced aging in the cancer cohort [Armenian et al.; Zhu et al.], consistent with overall greater comorbidity count (non-cancer + cancer) and shorter lifespan in the case cohort.

The patterns of Supplemental Table 1 for NBER present negative correlation between the dementia and cancer frequencies ( $r = -0.39$ ,  $p = 0.044$ ). In all studied categories the cancer mortality is significantly decreased as a function of behavioral or neurological impairments. For example, the hazard ratio of cancer mortality among the individuals with the congenital nervous system malformations is  $HR = 0.3$ ,  $p = 2.3 \times 10^{-34}$ . The similar hazard ratio for the injury-prone population is  $HR = 0.4$ ,  $p = 0$ , while for the never married cohort the  $HR = 0.9$ ,  $p = 2.25 \times 10^{-80}$ . For the cohorts suffering injury, trauma, accident and assault the dementia marker is elevated with the  $HR = 2.0$ ,  $p = 0$ . The effect of smoking is significant and meaningful biologically. As expected, smoking correlates with the increase of cancer mortality causes per a patient from 0.32 in control to 0.99 in the smoking cohort ( $HR = 3.1$ ,  $p = 0$ ). The effects of marital status are also noted, with singleness increased in the non-cancer control and married status enriched in cancer cohorts. The effects of educational achievement were considered earlier.

Figure 3A-B presents an additional validation of Wisconsin Longitudinal Study (WLS) results in the Kaiser Permanente Study of the Oldest Old [Kaiser] and Figure 3C-D presents the Chinese Longitudinal Healthy Longevity Survey (CLHLS) [CLHLS].

## Factor analysis of chronic disease and mortality in the National Alzheimer's Coordination Center dataset.

This section presents the analysis of the data in the version 3 of the National Alzheimer's Coordination Center dataset [URL, NACC]. The dataset is accumulated since 2004 and by the freeze date 03/2020 included > 150000 visits and > 42500 patients longitudinally monitored for the presence of comorbidities, including cognitive decline, cancer, diabetes, cardiovascular disease and more (Table 1). Versions 1 and 2 were excluded as not monitoring the entire list of comorbidities, together with the 25% of the profiles in the Version 3 that were incomplete. The remaining subset included 31495 doctor visits or telephone interviews. The dataset reports dozens of psychometric parameters and is relatively large, with the cancer cohort > 5000 visits and the control of > 25000. Thus, the expected statistical resolution is also high in NACC. The presence of dementia in the resulting trimmed dataset with the average age of 82 years was 24%, approaching the expected prevalence for the age [Bickel et al]. The results are presented in Table 1.

Table 1

t-stat profiles of the pre-morbidity factors (row 1) across comorbidity states (column 1). The left-most column 1 presents the list of outcomes, modelled by the factors preceding the onset of later-life morbidity. The upper row represents the traced factors: #1 – age; #2 – education; #3 – right-hand is dominant; #4 – height; #5 – BMI; #6 – weight; #7 – female gender; #8 – never married; #9 – divorced or never married; #10 – married; #11 – smoking measured as packs per day x years of smoking; race: #12- Hispanic; #13 – Caucasian; #14 – Black; #15 – Asian. The numbers are the t-stat values of the multiple regression models fitting the outcomes to the parameters, where the outcome is represented as (+1), while the absence is represented as (0).

FACTORS/OUTCOMES	#1	#2	#3	#4	#5	#6	#7	#8	#9	#10	#11	#12	#13	#14	#15
All-cause mortality	3.7	-8.2	1.0	-0.7	0.2	-2.3	-14.6	-1.3	4.8	0.4	0.0	-7.4	2.5	0.7	-0.5
Angina	2.5	-3.3	0.0	-0.6	1.6	-0.4	-7.4	-0.6	0.1	-1.3	1.9	-1.0	-4.6	-3.0	-4.6
Antipsychotics	5.9	-6.9	-2.8	-4.6	-4.1	4.5	-4.8	-0.7	-0.1	1.2	-0.5	1.6	1.1	0.1	0.5
Anxiety	4.4	-12.0	-2.3	-0.5	-0.8	-0.6	-2.3	0.8	-3.7	5.4	4.2	5.4	0.0	-2.3	-1.0
Arthritis	7.0	-1.2	2.0	-5.9	1.3	3.1	10.2	-3.2	3.8	-5.5	1.6	0.6	-2.7	-0.1	-5.4
Atrium fibrillation	-0.7	-1.9	1.5	1.5	-0.5	1.5	-7.2	-0.6	4.7	-2.7	-0.8	-7.0	2.3	0.4	0.8
B12 deficiency	0.4	-5.9	-1.7	1.0	0.9	-0.3	-0.8	-2.9	-0.8	-2.2	0.9	-0.5	1.1	0.9	0.2
Cancer	1.4	6.0	1.2	-0.5	-2.2	1.5	-4.0	-1.1	3.4	-1.3	1.2	-5.0	1.7	2.0	1.1
Cognitive decline	12.5	-27.8	-4.5	-1.6	-0.6	-3.2	-22.9	1.0	3.4	14.4	4.1	-1.8	4.0	1.8	2.0
Congestive heart failure	0.7	-3.3	0.7	-0.3	1.5	0.2	-5.4	-0.3	6.8	-1.4	-1.0	-1.6	-0.3	1.2	-0.6
Depression	4.3	-10.8	-3.6	-0.5	-0.7	0.8	-2.1	1.1	-2.8	-0.1	6.9	5.2	-1.4	-3.4	-2.0
Diabetes	4.9	-12.0	0.4	-4.0	2.8	4.7	-7.9	-1.4	2.8	-2.3	1.4	15.0	-6.4	-0.5	-0.6
Hypercholesterolemia	8.8	-3.1	1.6	-6.1	4.4	0.4	-17.9	-1.9	2.8	1.0	4.5	2.2	-0.7	0.0	0.7
Hypertension	12.5	-8.9	-0.4	-10.5	2.3	5.7	-17.3	-2.0	7.7	-2.7	2.6	1.8	-2.7	3.9	-0.5
Motor disorders	3.0	-14.4	-1.2	0.5	0.4	-1.2	-8.3	-1.0	-1.0	4.3	-0.2	-1.8	0.4	-1.0	-0.7
Myocardial infarction	4.8	-2.5	-0.9	-3.0	-1.7	2.7	-14.4	-2.3	1.7	-1.4	2.6	-1.0	-1.1	-1.0	-0.7
Pacemaker	1.2	-4.9	1.0	0.6	1.8	-1.8	-10.8	-0.1	3.6	-0.3	-2.6	-4.7	0.5	0.7	-0.1
Sleep apnea	6.3	4.0	-3.5	-8.2	-0.4	11.1	-16.3	-0.7	-3.0	-0.8	1.5	-1.5	-1.0	-1.8	-0.7
Thyroid	0.4	3.5	1.3	-2.6	0.6	0.7	22.9	-0.8	3.6	2.4	-0.3	-3.2	3.2	-1.1	1.4

Table 1 presents the t-stats of the multiple regression models computed for all-cause mortality and 20 comorbidities available in the NACC data. Vertical columns represent the t-stat profiles for the given factor across the disease models. The #2 (respondent's education) is the second most consistent factor negatively correlating with the presence of most of conditions, including mortality and cognitive decline. [Gottfredson LS, Deary]. However, the trend reverses for neoplasia (see also Figures 1, 2). The most consistent factors are gender (#7) and the chronological age (#1). For the elderly population of NACC, the t-stat effect of chronological age is not dominant and ranks the third after gender and education in its correlation with the health conditions. Across the 21 conditions of Table 1, divorce and singleness correlated positively with comorbidity, height correlated negatively, while weight and smoking correlated positively. *The effects of height, weight, unmarried status, and smoking were each less significant than the effect of education.* The results of this and the prior sections are consistent with cancer propensity accompanied by higher education as compared to other comorbidities at the same age and mortality rate.

## Cognitive status as a survival marker in aging and chronic disease.

Figure 4A-C presents the analysis of NACC organized in longitudinal format, with the timelines available for 42500 patients as of 3/2020. All versions and 151500 visits were included in the analysis, with the average 3-4 visits per a patient.

Figure 4A shows the effect of cognitive status and academic performance on the survival and cancer prevalence. In agreement with all prior results, cancer prevalence is decreased in the patients with the educational status < GED, while the highest prevalence is in the patients with the advanced degrees. The trend persists in the cognitively impaired and intact patients. Of note, the age when academic achievement is established temporally precedes the age of cancer development, *suggesting a putative causal relationship between the parameters of nervous system and tumorigenesis.* The annual probability of mortality  $H(T)$  decreases with educational performance for the cognitively normal individuals but does not form a trend for the cognitively impaired cohort. The 3-fold ratio of mortalities is observed between the cognitively impaired and intact strata, but the dynamic ratio decreases to 2-fold for the <GED cohorts.

Figure 4B shows the protective effect of retained cognitive normalcy on the survival in chronic disease. At the baseline ages 70.5-72, there is a dramatic difference between the  $H(T)$  values in the cognitively impaired and normal patients. The dynamic range is 6-fold for the patients

without cardiovascular disease, 3.5-fold for a single condition and 2-fold for two comorbidities. Analogously, similar dynamic ranges are observed for cancer, with the minimal range for the metastatic or multi-focal disease. The same trend exists for polypharmacy. This decrease of the dynamic range between the cognitively intact and impaired cohorts in the more challenging conditions is observed across all computations.

Figure 4C shows the analysis for the specific values of cognitive score and 4 ages, spanning the range between 66.5 and 93.5 years. In each bin of cognitive score, the values for H(T) follow the ages in the ascending order from left to right. The dynamic range is ~ 15 between the age 66.5 and 93.5 years at the top maximal cognitive score 30. The dynamic range becomes ~ 6 at the score 29, ~ 4.5 at 27-28, ~ 3.5 at 24-26, ~ 2.2 at 20-23 and only ~ 1.8 for the scores < 20. The absolute values of H(T) sharply depend on the value of cognitive score. The left-most bar of the plot is the H(T) for the 66.5 years old patients with the score 30 at the baseline and it is the lowest. The left-most bar for the score 29 indicates ~ 2.5 higher annual probability of mortality for the same age as compared to the score 30. The annual mortality rate doubles again for the bin 27-28 and doubles yet again for the bin 24-26 for the same age. At the age 93.5 the annual mortality rate still responds to the factor of cognitive score, but with lesser sensitivity as compared to the younger ages. The annual probability of mortality reaches ~ 0.26 for the 93.6 years old patients at the cognitive score 30 but increases to 0.58 for the score range < 20 at the same baseline age. By contrast, the H(T) is 0.016 for 66.5 years age at the cognitive score 30 and 0.32 at the cognitive score < 20, indicating a ~ 20-fold dynamic range. The annual mortality rate becomes age-independent with the cognitive loss (Figure 4C) or less age-dependent with accumulation of other senescence markers such as serious comorbidity (Figure 4B). Cognitive score exceeds both cardiovascular diseases and cancer as predictor of mortality (Figure 4B) and shows the effect commensurable with the effect of ~ 25 years of age (Figure 4C). The effects of academic performance in early life persist over lifetime and reflect on both the cancer prevalence and cognitive decline in later life (Figure 4A, Figure 5). The results of the section support a conclusion that the condition of central nervous system is rate-limiting in the progression to mortality, but other factors compete with the role of CNS at the extremely old ages or other sources of injury.

## Academic performance and cognitive status are inversely proportional to the rate of comorbidity accumulation.

Figures 5A and B present the results of analyzing the kinetics of changes in the level of aging markers as a function of academic performance or cognitive status. Such markers were cognitive score, the presence of cardiovascular disease and non-supplement (prescription) polypharmacy. One data point was measured at the beginning of follow up and the second point at the end, and the difference was related to the length of observation, producing the derivatives correlating with the biological aging rate.

Exploration of Figure 5A presents the aging-associated trends in the frequency of cardiovascular disease (CVD) as a function of cognitive score, with lower frequency of CVD associated with higher cognitive scores. Interestingly, the time-derivative of cardiovascular morbidity as well as time-derivative of prescription polypharmacy also follows the identical trend. Figure 5B presents the same for the dataset stratified by the educational achievement. Dramatic differences between “no GED” and “advanced degree” categories are observed for the dementia fractions reached by the baseline age (0.6 vs. 0.3) and the fraction of the “resisters”, defined as individuals retaining clinician-assessed cognitive norm through the entire follow up (0.19 vs 0.58). Analogously to Figure 5A, the rate of cognitive decline depends on the original value of cognitive score, accelerating for the “no GED” and “GED” categories. The statistically significant trends in the same direction are observed for H(T) and polypharmacy (CI95 are provided), although not so pronounced as the fractions of baseline dementia and percentage of “resisters” to dementia conversion. Each of these metrics is a surrogate of biological aging process and the data of Figure 5 support the conclusion that the increased stability and performance of central nerve system correlates with delayed aging rates.

The results produced in NACC were independently verified in NSHAP WAVE 2 (N = 3200), which is recruited randomly nationwide, while NACC is recruited based on the complains and volunteering (see Figure 6 below). The baseline ages in NSHAP were equalized in the  $68 \pm 1$  narrow range (N = 2000), to minimize the age-related biasing that can arise in the process of stratification. Figure 6A presents the trends analogous to all previously observed in NACC and other sources. Specifically, H(T) is strongly and inversely correlated to the MOCA values, producing > 4-fold dynamic range between the MOCA “1-14” and “26-30” subranges. The dynamic range in NSHAP is lower than that in NACC due to a smaller dataset size and higher noise-to-signal ratio. The MOCA score in late life in NSHAP strongly correlates the academic achievement in early life (the education code average is 1.5 in the MOCA “1-14” bin and 3.2 in the MOCA “26-30” bin). The fraction of cancer varies from 0.16 in the MOCA “1-14” bin to 0.28 in the MOCA “26-30” bin. Finally, the multimorbidity is ~ 1 condition/person in the “1-14” MOCA bin and 0.69 in the “26-30” bin.

Figure 6B compares the H(T) values at the different severity of health condition and values of MOCA score. An approximately 3-fold decrease in mortality is observed at 0-2 conditions, but the effect is less pronounced in the “>2” comorbidity range. Analogously to the observation for NACC, the impact of the cognitive score on H(T) exceeds the impact of one serious health condition.

## Retention of cognitive norm according to a clinical evaluation while experiencing decreased performance in cognitive score correlates with anomalously low mortality rates.

NACC provides multiple measures of cognitive state, in addition to MMSE and MOCA. The cognitive scores typically align with the objective diagnoses or functional norm, but not absolutely (Figure 6C). An assessment by a trained clinician is decisive and such scores are NACC NORM (clinical norm during all visits) and NACCUSDS (1 – norm, 2 – pre-MCI, 3 – MCI, 4-dementia). The discrepancies between the clinician-produced diagnoses and the diagnoses suggested by the cognitive scores are biologically important (below).

Figure 6C demonstrates that a small percent of dementia as defined by a clinician coexists at the baseline with the highest cognitive score 30, while a comparably tiny fraction of cognitive norm exists in the “<20” cognitive score stratum at the baseline. Still greater percentages of stable cognitive norm exist in the borderline score strata “20-23” and “24-26”.

We find especially interesting the anomalies that result from the superposition of the clinician-generated assessment of normalcy (NACCUSDS = 1 at the baseline and at the end of follow-up) and low cognitive score (MMSE/MOCA < 26) at the end of follow up. Such decrease of cognitive score places the patient into a risk category, but the clinician-assessed normalcy despite the increased risk suggests resistance to dementia conversion. These low-score resisters (termed +/- phenotype) differ from high score resisters (+/+ phenotype) or dementia converters (-/- phenotype). The data are presented in Figure 7.

Figure 7A shows dramatically different levels of annual mortality probability as a function of the phenotypes and follow up. The highest annual probability is observed in dementia, followed by the high score resisters. Abstraction of cardiovascular morbidity decreases the annual mortality rates in the high score resisters, but the previous trend remains. The bottom graph in Figure 7A refers to the low score resisters and demonstrates the lowest mortality rate. Remarkably, in the subset 7 years after the baseline (the age of 85 years), the  $H(T)$  is  $\sim 0.015$ , that is the value corresponding to the general population annual mortality rate at 66 years. The annual mortality rate increases to 0.025 by 90 years, still maintaining the  $\sim 20$  years gap with the average population. Figure 7B presents the fraction of cardiovascular disease at baseline. Cardiovascular disease is maximal in the shortest follow up interval and in the dementia converter phenotype. Cardiovascular disease is lower in the high-score resisters and much lower in the low-score resisters, suggesting the explanation of the lower mortality and resistance to dementia conversion. However, as Figure 7A demonstrates, the complete exclusion of cardiovascular morbidity in the high-score resisters produces a population with the annual mortality still exceeding that of low-score resisters. Figure 7C demonstrates that the low-score resisters are biologically distinct from both dementia converters and high-score resisters. The latter produce closely matching attrition profiles (the numbers of the patients leaving the study at a particular year of follow up) with the tangent  $\sim -0.26$ . By contrast, the low-score resisters demonstrate slow attrition profile with the tangent  $\sim -0.15$ . This tangent is proportional to the exponential Gompertz constant beta [Ricklefs et al.], suggesting that the low-score resisters age at the rate of  $\sim 0.6$  of the general population, during at least a segment of overall lifespan. The relatively reduced fraction of cardiovascular disease is likely not a cause but a consequence of the slow-aging phenotype, which is also characterized by high tolerance to the reduction of cognitive score without developing clinical dementia. The exclusion of cardiovascular morbidity shown in Figure 7A is expected to change the attrition profile in Figure 7C if cardiovascular health was the primary factor in these patterns. However, the profile after exclusion remains unchanged and still differs from that of the low-score resisters.

## Life-expectancy after the baseline age is proportional to the baseline cognitive score.

NACC recruits the patients and relatives since 2004 up to the present time, with the median year of recruitment being 2011. The patients are observed until the accumulated disability makes further collaboration unfeasible or until the patients die. The follow-up intervals are variable and reflect the baseline state of health and potential longevity of an individual. The individuals with longer follow up intervals are healthier and achieve longer lifespans. Figure 7 indicates that the mortality rate disproportionally decreases in the longer follow up cohorts, but this observation can be an artifact. The study used in this report was released in the March of 2020 and in longer follow ups (ending closely to the release date) the decedents do not have time to accumulate. Thus, the direct mortality measurement is not appropriate, and instead we applied the proxy markers such as cognitive state, polypharmacy, and cardiovascular disease, being all linked as benchmarks of aging [Franceschi C et al.].

Figure 8A shows that the follow up length correlates to the baseline value of cognitive score. The shorter follow ups (1-2 years) associate with lower baseline cognitive scores 24-25, while the longer follow ups (9-10 years) correspond to almost maximal cognitive scores of 29.5. The final cognitive score before the attrition is almost constant in all cohorts and is about  $\sim 20$ , considered a borderline value between mild

cognitive impairment and dementia. The baseline polypharmacy is lower in the longer-observed individuals, but the final polypharmacy is higher in the older individuals at longer follow ups. Figure 8B shows the time-derivatives of cardiovascular disease frequency, polypharmacy, cognitive score aligned with the annual mortality H(T). All derivatives form a similar profile, being 3-fold higher for the shorter follow-ups. The H(T) profile is confirmed by that of the surrogates. The result of Figure 8 show that once the baseline level of senescence is high, further senescence proceeds with acceleration. There is the final level of neurological and non-neurological damage that leads to attrition from the study that precedes mortality by 0-3 years. The decline of cognitive score to ~ 20, the presence of cardiovascular disease in ~ 60-90% of the cohort and the polypharmacy in the range 4.6-5.7 on average define this threshold. The extent of non-neurological damage is higher in longer-living patients, suggesting the reason why H(T) stops to respond to cognitive status in the oldest old, as shown previously. Not only the protective effect of relatively healthy nervous system weakens with age, but the senescence pressure increases exponentially, as suggested in Figure 8B.

## Discussion

This discussion attempts to rationalize from common positions the seemingly disparate lines of evidence revolving around cognitive state and educational performance. The aspects that need rationalizing are the following:

- a) Stronger educational performance in early life and higher cognitive score in later life positively correlates with the presence of cancer [Larsen et al., Coughlin et al., Dong et al., Savijarvi et al.], but negatively correlates with the presence of other comorbidities. [Gottfredson et al], [Deary et al.], [Brown et al], and [Zeng].
- b) The present or future cancer patients retain higher level of performance, physically and mentally as compared with the same age peers suffering from non-cancer chronic disease with comparable mortality [Nudelman et al., Shafi et al; Zhang et al.].
- c) Cancer proceeds more aggressively in more educated individuals (Figure 1-3), the link between cancer and the status of nervous system is biological [Mauffrey et al., Dart, Cervantes-Villagrana et al, Xing et al., Kallay et al., Zhuo et al, Yuan et al., Van der Willik et al., Linni et al.].
- d) Cognitive status correlates with longevity and cognitive stability is protective in all serious chronic conditions. However, this protective effect decreases with age or with the extent of pre-existing damage. Cognitive status is a rate-limiting parameter for mortality (Figures 4, 8).
- e) The aging rate is delayed in more educated and cognitively stable individuals [Clouston et al., Deary et al., Figure 5]. It is especially delayed in the individuals resistant to dementia conversion while being formally in a high-risk group (Figure 7).
- f) Longer follow ups correspond to slower senescence observed at the baseline and the senescence accelerates in the presence of the pre-existing decline [Elliott et al.]. The ratio of neurological to non-neurological damage is lower in longer-living phenotypes (Figure 8).

We proposed a unifying hypothesis that explains the data of this report from the common positions.

Nerve system maintains regenerative potential in traumas (Knox et al., Boilly et al.). In fact, denervated organs fail to regenerate in multiple animal models (Knox et al, Boilly et al.). Denervation of the primary tumor suppresses cancer growth and metastasis [Zhao et al., Magnon et al.]. Nerve system acts through multiple molecular mechanisms such as neuropeptides, neurotransmitters, morphogens, mitogenic growth factors. In amphibian limb regeneration, these factors attract and activate the blastema (mobilized progenitor cells undergoing further differentiation into the organ components) – and the regeneration block that accompanies denervation depends on the disruption of blastema mobilization [Satoh et al.]. In mammals, whole organ regeneration is not observed, but partial regeneration follows a similar mechanism, beginning with CNS-mediated stem cell mobilization [Borlongan et al.]. CNS also provides routine, non-trauma maintenance of stem-cell activity. For example, spinal cord injury causes chronic bone marrow failure, suggesting that regular functioning of bone marrow depends on constant CNS stimulation [Carpenter et al.]. Circulating progenitor cells (CPC) are mobilized from the marrow niches by stress, trauma, inflammatory cytokines, and direct non-traumatic circadian brain signaling [Mendez-Ferrer et al.]. Reciprocally, the increase in the titer of the circulating peripheral blood progenitor cells stimulates CNS and reverses advanced cognitive decline [He et al.].

Senescence and trauma share pro-inflammatory pathways, demonstrating synergy [Sullivan et al.], *We propose that senescence is countered in mammals (and perhaps other taxa) by a mechanism analogous to the bone marrow activation by the intact spinal cord described in Carpenter et al.* Specifically, central nervous system in its healthy state induces a baseline level of stem cell mobilization and activation. The secretome of these stem cells is anti-inflammatory and pro-survival and they permeate all vital organs, while also being present in peripheral circulation [Lunyak et al.]. The circulating progenitor cell (CPC) titer correlates with systemic stem activity and the endogenous regenerative potential. The circulating progenitor titer is not the only parameter characterizing the endogenous regenerative potential that also includes responsiveness to the mobilization stimuli and potency of the stem cell signaling [Zhu et al., Phan et al.]. The CPC do not exclusively

originate in bone marrow, but derive from diverse niches such as small intestine, liver, blood vessel walls and in some contexts these non-marrow subsets provide the bulk of regeneration in the damaged organs [Aicher et al.].

These circulating progenitor cell titers correlate with memory, posterior cortical thickness, and hippocampal perfusion [Nation et al.]. Higher CPC levels are associated with the reduced risk of cognitive decline [Hajjar et al.]. The reduced circulating progenitor mononuclear CD34+ cell or CD133 counts are associated with the risk of death in cardiovascular disease, suggesting that impaired endogenous regeneration relates to increased mortality [Patel et al., Rigato et al.]. The CPC levels vary with the individual factors that contribute to mortality or survival, for example they increase count with smoking cessation [Kondo et al.] and decrease in severe pulmonary disease [Fadini et al.]. The CD34+ CPC retained their prognostic value as a biomarker of longevity at the ages when other factors such as smoking or cardiovascular disease stopped to be predictive [Mandraffino et al.]. At the same time, the increase of circulating progenitors is observed in hepatic and breast cancers [Zahran et al.; Montaser et al.]. Progenitor senescence parallels decrease in cancer prevalence and aggressiveness in the oldest old [Pedersen et al., Pavlidis et al.]. The factors listed in the Table 1 parallel the circulating progenitor activity, with cardiovascular disease, obesity, diabetes, and cognitive decline negatively correlating with CD34+ PCP levels, while cancer correlates positively.

The above-described scenario explains the disappearance of mortality dependence on age at lower cognitive scores < 20, described in Figure 4. The telomere length is known to decrease sharply in dementia [Koh et al.]. The critical level of senescence incompatible with life is reached earlier when the regenerative effect of nervous system is weak (Figure 8). The neurogenic regenerative effect postpones the terminal aging stage (Figure 8).by impacting the general aging rate (Figure 5). The individuals with sharply decreased cognitive scores demonstrate exhausted overall vitality, accompanied by “exploding” morbidity [Franceschi C et al.] and this exhaustion can take place at various ages (Figure 4, 8). The effects of senescence are self-reinforcing through the autocrine loop mechanisms and the presence of chronic disease, advanced chronological age or pre-existing cognitive decline share the high level of pre-existing senescence, explaining the patterns of Figure 4.

The trophic effects of nervous system, preventing functional decline of multiple organs may also be direct and not mediated by the progenitor cells. The retention of active acetylcholine receptors prevents the atrophy of skeletal muscles and favor reinnervation in the isolated skeletal myofibers [Cisterna et al.]. Similar direct trophic pathways are mediated by neuropeptides, with glia initiating long-range activation of the endoplasmic reticulum UPR (UPRER) in distal cells to coordinate stress resistance and longevity in *C. elegans* [Miklas et al.]. Another effect in the round worms is secretion of miRNA-71 by the olfactory neurons regulating protein turnover in the peripheral tissue and longevity [Finger et al.]. Similar pathways may exist in mammals and provide the stimulating multimodality synergizing with the stem cell mobilization mechanism.

One mammalian model – naked mole rat (NMR) – especially resonates with the data and hypothesis of this report. The mole rat lives in hypoxic and hypothermic conditions and displays - for most of its lifespan - a constant annual probability of mortality  $H(T)$ , departing from the Gompertz law of exponential  $H(T)$  profile [Ruby et al.]. At the same time, the NMR can experience cellular senescence at the extreme old age [Zhao et al], suggesting that the unique  $H(T)$  profile and longevity is the result of a powerful anti-senescence mechanism, postponing the dynamics that develops earlier in shorter-living species. The lifespan of this small animal exceeds that of comparably sized rodents by more than an order of magnitude [Ruby et al.]. The organism is exceptionally resistant to cancer, preventing its development by multiple mechanisms [Miyawaki S., Hadi et al.]. Our hypothesis predicts that NMR relies on anomalously high baseline progenitor cell activity, mobilized by the CNS, and augmented by the reduced brain aging rate as the hypothetical anti-aging mechanism. Such method of postponing senescence develops spontaneously as a byproduct in hypoxic hypercapnic conditions stimulating pluripotency and aggressive tumor development - if not countered by evolution [Wei et al., Tolstun et al.]. It is unclear otherwise *why NMR needs to be cancer-resistant in the absence of natural exposure to radiation or carcinogens*, but the above interpretation provides a rationale. Longevity evolves as a byproduct of the increased stem and telomerase activity [Leonida et al], induced by hypothermia, hypoxia, and hypercapnia of the flooded NMR burrow habitats. Small rodents are known to express telomerase in the somatic tissues and 90% of ordinary mice dies in captivity of cancer [Gorbunova et al.]. NMR also expresses telomerase in somatic tissues [Gorbunova et al.], and this original ability combined with cancer control could be evolutionally exploited to develop the anomalous longevity of mole rats, also benefiting from the social structure selecting for greater stability of colonies with longer lasting individuals. Indeed, dramatically elevated germline activity is observed in this animal model [Place et al.], together with the extraordinary neuronal plasticity and juvenile pluripotency markers persisting in adult brain [Orr et al., Penz et al.]. The brain in this animal structurally resembles a primate's more than a rodent's [Orr et al.], in contrast with a narrow ecological niche and relatively non-stimulating lifestyle. However, the lifespan-regulating role of such brain – and not information processing – would justify its plasticity, also induced by the feedbacks from the hypoxia-adapted pro-pluripotency environment of this organism.

The human-centered phenomena described in this article may be the root analogues of mole rat adaptations, inherent to other mammalian species. Humans do respond to hypoxia with increased longevity [Zubieta-Calleja et al.], proportional to the altitude. A paradoxical hypoxia-like effect of hyperbaric oxygenation leads to telomere lengthening by 20% and at least temporary reversal of aging in some lineages

[Hachmo et al.]. Adult spermatozoids in the older men show telomere lengthening as compared to younger ages and this lengthening carries over to the offspring [Stindl et al.], suggesting anti-senescence in fully differentiated human cells, perhaps through regulated telomerase activation. Humans are under less pressure to develop the additional anti-cancer mechanisms as compared to mole rats, because human survival does not depend on the primary adaptation to extreme hypoxia and the secondary adaptation to the aggressive clonal expansion that can follow a generalized hypoxia response. On the contrary, *by relaxing cancer controls, humans benefited from higher mobilized stem activity* that is supportive of mental processes, physical endurance, regeneration, immunity, and socialization. The resulting longevity further evolved as a stabilizer of small groups of human ancestors and as an enhancer of individual performance in the survival game of a creature mostly devoid of natural weapons.

The results of our study can be practically applied in development of risk markers by comparing the molecular profiles of the individuals with the declining and intact cognitive scores, combined with the clinician's evaluation (Figure 7). Once mortality risk is predicted by the cognitive profile of a person, the individual is assigned to the case or control class, biological fluids are extracted and analyzed to define the molecular markers/mediators of enhanced survival or mortality risk.

## Methods

### Data sources

The NBER (National Bureau of Economic Research) database, Multiple Causes of Death [NBER] contains scanned data profiles obtained from death certificates, including age, gender, education, demographic and family status of the decedent, number of diseases, ICD-10/358 codes of the individual diseases, and the order in which they are considered. The database includes data from across the USA since 1959 with more than 70 million decedent profiles as of 2016. The coverage for this project was limited to 1999-2017. The ICD-10 code G30.9 was selected to identify Alzheimer's disease; F02\* and F03\* were used for other forms of dementia, excluding alcohol-induced; I10-I15\*, I20-I25\*, I26-I28\*, and I30-I52\* were selected for cardiovascular disease; M13\*, M15-M19\*, and M02-M09\* were selected for arthropathies; E10-E14\* were used for diabetes; C\* was used for malignancies.

The National Social Life, Health, and Aging Project (NSHAP) Waves 1 and 2 [NSHAP] are affiliated with the Inter-university Consortium for Political and Social Research (ICPSR). The longitudinal dataset (>3000 patients) at the average ages ~ 72 years provides information about pharmaceutical exposure, comorbidity presence and all-cause mortality. Cancer localizations, cognitive scores, and mortality/lifespan data are provided. The individual cognitive scores in NSHAP II combine in the MOCA index.

The Kaiser Permanente Study of the Oldest Old, 1971-1979 and 1980-1988 (California) is a longitudinal observation study of the elderly > 65 years old (>5900 patients) with 35 clinician-diagnosed conditions that were carefully monitored, and education, lifestyle, cognitive status, disability, institutionalization, hospital visits, cancer as well as anatomical localizations are available [KAISER].

The Irish Longitudinal Data on Aging (TILDA) project is a longitudinal study of individuals above 50 years of age in Ireland [TILDA], which was conducted from 2009 to 2015 in 3 waves. Waves 1-3 were analyzed for this project; the averaged Mini Mental State Examination (MMSE) scores were computed. The education, income, lifestyle, disability, hospitalizations, comorbidity, childhood, marriage data are provided, while the presence of cancer was deduced from the medical insurance information for > 6500 respondents in this report. [TILDA].

The Wisconsin Longitudinal Study (WLS, 1957-2007) is available as a part of the project RELATE [RELATE] contributing the US component, alongside with China, Africa, Latin America, India and Russia. WLS provides the detailed information regarding comorbidity, mortality, education, income, lifestyles, childhood. All respondents to the survey conducted in 2003-2004 are of the same age in the 64-66 years range, simplifying the analysis for > 6000 respondents to the 2003-2004 survey included in this report.

The National Health Interview Survey, 1994: Second Longitudinal Study on Aging, Wave 3, 2000 (NHIS) begins in 1994 at the baseline, with two questionnaires processed in 1996 and 1998. The comorbidity, mortality, hospitalization, institutionalization, disability, military service, lifestyles are available for > 7800 respondents with the average age 78 years [NHIS].

The Chinese Longitudinal Healthy Longevity Survey (CLHLS) provides information on health status and quality of life of the elderly aged 65 and older in 22 provinces of China in the period 1998 to 2012. The CLHLS provides information on the health, socioeconomic characteristics, family, lifestyle, and demographic profile of this aged population. Data are provided on respondents' health conditions, daily functioning, self-perceptions of health status and quality of life, life satisfaction, mental attitude, and feelings about aging. Respondents were asked about their diet and nutrition, use of medical services, and drinking and smoking habits. They were also asked about their physical activities, reading habits, television viewing, and religious activities, and were tested for motor skills, memory, and visual functioning [CLHLS].

Midlife in the United States (MIDUS 1), 1995-1996 is a collaborative, interdisciplinary investigation of patterns, predictors, and consequences of midlife development in the areas of physical health, psychological well-being, and social responsibility. The WAVES 2 and 3 of the study were integrated in the single dataset. The data reflect comorbidities, exercise, personal character, lifestyle, employment status, education, income, childhood status [MIDUS].

The datasets in the original form are available at the sources [ICSPR] and are deposited in the processed form to the website (See the List of Files).

The National Alzheimer's Coordination Center dataset [NACC] is available based on a collaborative agreement. This is a longitudinal multicenter clinical study of > 40000 patients and controls, addressing cognitive status, health, lifestyles, demographics. The dataset provides extensive psychometric data and use of pharmaceuticals.

The data and the accompanying workbooks in PDF form are available at NBER, NACC and ICPSR depositories [NBER, NACC, ICPSR]. Also, ICPSR offer online analysis of the features presented in the datasets. The processed data of the analysis are provided in the Supplemental Table 2, where the links lead to the Excel datasets which are further annotated. The datasets present the original data combined with the stratification or regression model analysis and the figures used in the main manuscript.

## Data stratification analysis

The data were categorized in groups based on a common label, for example "cancer" and "control". The groups were further stratified based on the target criteria. In each stratum, the averages were computed and plotted. The variations were computed by producing random groups of constant size, tracking the averages of the labels, and computing standard deviations across the groups. Variations were pro-rated to the groups of different size by the formula:

$$S_1 = S_2 \times (N_2/N_1)^{0.5} \quad (2)$$

Where  $S_1$  is variation in the standardized random groups of the size  $N_1$ ,  $S_2$  is variation at the arbitrary groups of the size  $N_2$ .

## Linear regression model analysis

General introduction to the multiple linear regression methods is provided in [Rencher et al.]. The software LINEST accepts 15 independent variables and returns the predictor, variation, regression coefficient, t-test, p-value associated with the regression coefficient and the ratio of the regression coefficient to the variation, termed "t-statistics", as well as confidence interval. The "features" and "outcome" columns are designated in the data files, to be read into the appropriate software input fields.

The predictor columns were examined for the missing values and if identified the averages for the column were imputed. Only the columns with all non-empty elements were accepted by the LINEST. The resulting final predictor incorporating all sub-models was ranked, the rank was divided in the percentile bins and the values of all factors of interest (parameters and outcomes) were computed in the percentile bins of the rank (95-100%, 90-94%, 85-89% etc.). Such values are plotted as a function of the predictor percentile.

## Declarations

## AUTHOR CONTRIBUTIONS

AM initiated the study, analyzed the data, wrote the draft of the manuscript text and prepared the initial figures 1–8.

## COMPETING INTERESTS STATEMENT

The author declares no competing interests.

## DATA AVAILABILITY STATEMENT

All data generated or analyzed during this study are included in this published article (and its Supplementary Information files).

## References

1. Beard GM. The Longevity of Brain-Workers. *Public health papers and reports*. 1873;1:54.
2. Minias P, Podlaszczuk P. Longevity is associated with relative brain size in birds. *Ecology and Evolution*. 2017 May;7(10):3558-66.
3. Rushton JP. Brain size as an explanation of national differences in IQ, longevity, and other life-history variables. *Personality and Individual Differences*. 2010 Jan 1;48(2):97-9.
4. Peters A, Hitze B, Langemann D, Bosy-Westphal A, Müller MJ. Brain size, body size and longevity. *International journal of obesity*. 2010 Aug;34(8):1349-52.
5. Pontzer H, Brown MH, Raichlen DA, Dunsworth H, Hare B, Walker K, Luke A, Dugas LR, Durazo-Arvizu R, Schoeller D, Plange-Rhule J. Metabolic acceleration and the evolution of human brain size and life history. *Nature*. 2016 May;533(7603):390-2.
6. Gottfredson LS, Deary IJ. Intelligence predicts health and longevity, but why? *Current Directions in Psychological Science*. 2004 Feb;13(1):1-4.
7. Deary I. Why do intelligent people live longer? *Nature*. 2008 Nov;456(7219):175-6.
8. Deary IJ, Batty GD, Pattie A, Gale CR. More intelligent, more dependable children live longer: A 55-year longitudinal study of a representative sample of the Scottish nation. *Psychological Science*. 2008 Sep;19(9):874-80.
9. Mattson MP, Duan W, Maswood N. How does the brain control lifespan? *Ageing research reviews*. 2002 Apr 1;1(2):155-65.
10. Pandit M, Behl T, Sachdeva M, Arora S. Role of brain derived neurotrophic factor in obesity. *Obesity Medicine*. 2020 Mar 1;17:100189.
11. Imai SI, Guarente L. It takes two to tango: NAD<sup>+</sup> and sirtuins in aging/longevity control. *npj Aging and Mechanisms of Disease*. 2016 Aug 18;2(1):1-6.
12. Miklas JW, Brunet A. Support cells in the brain promote longevity. *Science*. 2020 Jan 24;367(6476):365-6.
13. Bussian TJ, Aziz A, Meyer CF, Swenson BL, van Deursen JM, Baker DJ. Clearance of senescent glial cells prevents tau-dependent pathology and cognitive decline. *Nature*. 2018 Oct;562(7728):578-82.
14. Xu M, Pirtskhalava T, Farr JN, Weigand BM, Palmer AK, Weivoda MM, Inman CL, Ogrodnik MB, Hachfeld CM, Fraser DG, Onken JL. Senolytics improve physical function and increase lifespan in old age. *Nature medicine*. 2018 Aug;24(8):1246-56.
15. He Y, Jin X, Wang J, Meng M, Hou Z, Tian W, Li Y, Wang W, Wei Y, Wang Y, Meng H. Umbilical cord-derived mesenchymal stem cell transplantation for treating elderly vascular dementia. *Cell and tissue banking*. 2017 Mar 1;18(1):53-9.
16. Cole JH, Ritchie SJ, Bastin ME, Hernández MV, Maniega SM, Royle N, Corley J, Pattie A, Harris SE, Zhang Q, Wray NR. Brain age predicts mortality. *Molecular psychiatry*. 2018 May;23(5):1385-92.
17. Tara S, Krishnan LK. Differentiation of circulating neural progenitor cells in vitro on fibrin-based composite-matrix involves Wnt- $\beta$ -catenin-like signaling. *Journal of cell communication and signaling*. 2019 Mar 1;13(1):27-38.
18. Mauffrey P, Tchitchek N, Barroca V, Bemelmans A, Firlej V, Allory Y, Roméo PH, Magnon C. Progenitors from the central nervous system drive neurogenesis in cancer. *Nature*. 2019 May; 569(7758):672.
19. Dart A. Nervous tumours. *Nature Reviews Cancer*. 2019 May 28:1.
20. Nudelman KN, McDonald BC, Lahiri DK, Saykin AJ. Biological Hallmarks of Cancer in Alzheimer's Disease. *Molecular neurobiology*. 2019 Apr 16:1-5.
21. Shafi O. Inverse relationship between Alzheimer's disease and cancer, and other factors contributing to Alzheimer's disease: a systematic review. *BMC neurology*. 2016 Dec;16(1):236.
22. Zhang Q, Guo S, Zhang X, Tang S, Shao W, Han X, Wang L, Du Y. Inverse relationship between cancer and Alzheimer's disease: a systemic review meta-analysis. *Neurological Sciences*. 2015 Nov 1;36(11):1987-94.
23. Van der Willik KD, Schagen SB, Ikram MA. Cancer and dementia: Two sides of the same coin? *European journal of clinical investigation*. 2018 Nov;48(11):e13019.
24. Lanni C, Masi M, Racchi M, Govoni S. Cancer and Alzheimer's disease inverse relationship: an age-associated diverging derailment of shared pathways. *Molecular Psychiatry*. 2020 May 7:1-6.
25. Rehm J, Shield KD, Weiderpass E. Alcohol consumption. A leading risk factor for cancer. *Chemico-Biological Interactions*. 2020 Oct 1:109280.
26. Early Life and Aging Trends and Effects (RELATE): A Cross-National Study. <https://www.icpsr.umich.edu/web/ICPSR/studies/34241>.
27. Ritchey MD, Wall HK, George MG, Wright JS. US trends in premature heart disease mortality over the past 50 years: Where do we go from here? *Trends in cardiovascular medicine*. 2019 Sep 27.
28. The Irish Longitudinal Study on Ageing (TILDA). <https://www.icpsr.umich.edu/icpsrweb/NACDA/series/726> (2018).

29. Sun M, Wang Y, Sundquist J, Sundquist K, Ji J. The Association Between Cancer and Dementia: A National Cohort Study in Sweden. *Frontiers in oncology*. 2020 Feb 4;10:73.
30. Hayes-Larson E, Ackley SF, Zimmerman SC, Ospina-Romero M, Glymour MM, Graff RE, Witte JS, Kobayashi LC, Mayeda ER. The competing risk of death and selective survival cannot fully explain the inverse cancer-dementia association. *Alzheimer's & Dementia*. 2020 Sep 3.
31. National Bureau of Economic Research. <http://www.nber.org/data/vital-statistics-mortality-data-multiple-cause-of-death.html> (2018).
32. ICPSR (<https://www.icpsr.umich.edu/web/pages/ICPSR/index.html>)
33. National Social Life, Health, and Aging Project (NSHAP): Wave 2 and Partner Data Collection. <https://www.icpsr.umich.edu/icpsrweb/NACDA/studies/34921> (2018).
34. National Health Interview Survey, 1994: Second Longitudinal Study on Aging, Wave 3, 2000 <https://www.icpsr.umich.edu/web/ICPSR/studies/3807>.
35. Midlife in the United States (MIDUS 1), 1995-1996 (ICPSR 2760) <https://www.icpsr.umich.edu/web/ICPSR/studies/2760>.
36. Kruk J, Aboul-Enein BH, Bernstein J, Gronostaj M. Psychological Stress and Cellular Aging in Cancer: A Meta-Analysis. *Oxidative Medicine and Cellular Longevity*. 2019 Nov 13;2019.
37. Klein WM, Jacobsen PB, Helzlsouer KJ. Alcohol and cancer risk: clinical and research implications. *Jama*. 2020 Jan 7;323(1):23-4.
38. Armenian SH, Gibson CJ, Rockne RC, Ness KK. Premature aging in young cancer survivors. *JNCI: Journal of the National Cancer Institute*. 2019 Mar 1;111(3):226-32.
39. Zhu J, Wang F, Shi L, Cai H, Zheng Y, Zheng W, Bao P, Shu XO. Accelerated aging in breast cancer survivors and its association with mortality and cancer recurrence. *Breast Cancer Research and Treatment*. 2020 Feb 4:1-1.
40. Kaiser Permanente Study of the Oldest Old, 1971-1979 and 1980-1988: [California]. <https://www.icpsr.umich.edu/icpsrweb/NACDA/studies/4219> (2018).
41. Chinese Longitudinal Healthy Longevity Survey (CLHLS), 1998-2012 (ICPSR 36179) <https://www.icpsr.umich.edu/web/ICPSR/studies/36179>.
42. Franceschi C, Garagnani P, Morsiani C, Conte M, Santoro A, Grignolio A, Monti D, Capri M, Salvioli S. The continuum of aging and age-related diseases: common mechanisms but different rates. *Frontiers in medicine*. 2018 Mar 12;5:61.
43. NACC project URL: [https://www.alz.washington.edu/WEB/researcher\\_home.html](https://www.alz.washington.edu/WEB/researcher_home.html)
44. Bickel H, Hendlmeier I, Heßler JB, Junge MN, Leonhardt-Achilles S, Weber J, Schäufele M. The Prevalence of Dementia and Cognitive Impairment in Hospitals: Results from the General Hospital Study (GHoSt). *Deutsches Ärzteblatt International*. 2018 Nov;115(44):733.
45. Stallard E. Compression of morbidity and mortality: new perspectives. *North American Actuarial Journal*. 2016 Oct 1;20(4):341-54.
46. Chiu CT. Advanced Education and Mortality Compression in the United States. *EurAmerica*. 2017 Jun 1;47(2).
47. Ricklefs RE, Scheuerlein A. Biological implications of the Weibull and Gompertz models of aging. *The Journals of Gerontology Series A: Biological Sciences and Medical Sciences*. 2002 Feb 1;57(2):B69-76.
48. Lesuffleur T, Coldefy M, Rachas A, Gastaldi-Ménager C, Tuppin P. Associations between mental illnesses and acute cardiovascular events and cancers in France in 2016. *European Journal of Public Health*. 2019 Nov 1;29(Supplement\_4):ckz187-194.
49. Larsen IK, Myklebust TÅ, Babigumira R, Vinberg E, Møller B, Ursin G. Education, income and risk of cancer: results from a Norwegian registry-based study. *Acta Oncologica*. 2020 Sep 11:1-8.
50. Coughlin SS. Social determinants of breast cancer risk, stage, and survival. *Breast Cancer Research and Treatment*. 2019 Oct 1:1-2.
51. Dong JY, Qin LQ. Education level and breast cancer incidence: a meta-analysis of cohort studies. *Menopause*. 2020 Jan 1;27(1):113-8.
52. Savijärvi S, Seppä K, Malila N, Pitkaniemi J, Heikinen S. Trends of colorectal cancer incidence by education and socioeconomic status in Finland. *Acta Oncologica*. 2019 Nov 2;58(11):1557-63.
53. Brown DC, Hayward MD, Montez JK, Hummer RA, Chiu CT, Hidajat MM. The significance of education for mortality compression in the United States. *Demography*. 2012 Aug 1;49(3):819-40.
54. Zeng X, Liu J, Tao S, Hong HG, Li Y, Fu P. Associations between socioeconomic status and chronic kidney disease: a meta-analysis. *J Epidemiol Community Health*. 2018 Apr 1;72(4):270-9.
55. Cervantes-Villagrana RD, Albores-García D, Cervantes-Villagrana AR, García-Acevez SJ. Tumor-induced neurogenesis and immune evasion as targets of innovative anti-cancer therapies. *Signal transduction and targeted therapy*. 2020 Jun 18;5(1):1-23.
56. Xing W, Chen DT, Pan JH, Chen YH, Yan Y, Li Q, Xue RF, Yuan YF, Zeng WA. Lidocaine induces apoptosis and suppresses tumor growth in human hepatocellular carcinoma cells in vitro and in a xenograft model in vivo. *Anesthesiology: The Journal of the American Society of Anesthesiologists*. 2017 May 1;126(5):868-81.

57. Kallay L, Keskin H, Ross A, Rupji M, Moody OA, Wang X, Li G, Ahmed T, Rashid F, Stephen MR, Cottrill KA. Modulating native GABA A receptors in medulloblastoma with positive allosteric benzodiazepine-derivatives induces cell death. *Journal of neuro-oncology*. 2019 May 1;142(3):411-22.
58. Zhuo C, Xun Z, Hou W, Ji F, Lin X, Tian H, Zheng W, Chen M, Liu C, Chen C, Wang W. Surprising anticancer activities of psychiatric medications: old drugs offer new hope for patients with brain cancer. *Frontiers in pharmacology*. 2019;10:1262.
59. Yuan SY, Cheng CL, Ho HC, Wang SS, Chiu KY, Su CK, Ou YC, Lin CC. Nortriptyline induces mitochondria and death receptor-mediated apoptosis in bladder cancer cells and inhibits bladder tumor growth in vivo. *European Journal of Pharmacology*. 2015 Aug 15;761:309-20.
60. Clouston SA, Smith DM, Mukherjee S, Zhang Y, Hou W, Link BG, Richards M. Education and cognitive decline: An integrative analysis of global longitudinal studies of cognitive aging. *The Journals of Gerontology: Series B*. 2020 Aug 13;75(7):e151-60.
61. Knox SM, Lombaert IM, Haddox CL, Abrams SR, Cotrim A, Wilson AJ, Hoffman MP. Parasympathetic stimulation improves epithelial organ regeneration. *Nature communications*. 2013 Feb 19;4(1):1-7.
62. Elliott ML, Belsky DW, Knodt AR, Ireland D, Melzer TR, Poulton R, Ramrakha S, Caspi A, Moffitt TE, Hariri AR. Brain-age in midlife is associated with accelerated biological aging and cognitive decline in a longitudinal birth cohort. *Molecular Psychiatry*. 2019 Dec 10:1-0.
63. Boilly B, Faulkner S, Jobling P, Hondermarck H. Nerve dependence: from regeneration to cancer. *Cancer Cell*. 2017 Mar 13;31(3):342-54.
64. C.M. Zhao, Y. Hayakawa, Y. Kodama, S. Muthupalani, C.B. Westphalen, G.T. Andersen, A. Flatberg, H. Johannessen, R.A. Friedman, B.W. Renz, et al. Denervation suppresses gastric tumorigenesis *Sci. Transl. Med.*, 6 (2014), p. 250ra115
65. Magnon, S.J. Hall, J. Lin, X. Xue, L. Gerber, S.J. Freedland, P.S. Frenette Autonomic nerve development contributes to prostate cancer progression *Science*, 341 (2013), p. 1236361
66. Satoh A, Mitogawa K, Makanae A. Nerve roles in blastema induction and pattern formation in limb regeneration. *International Journal of Developmental Biology*. 2018 Sep 14;62(9-10):605-12.
67. Borlongan CV. Bone marrow stem cell mobilization in stroke: a 'bonehead' may be good after all!. *Leukemia*. 2011 Nov;25(11):1674-86.
68. Carpenter RS, Marbourg JM, Brennan FH, Mifflin KA, Hall JC, Jiang RR, Mo XM, Karunasiri M, Burke MH, Dorrance AM, Popovich PG. Spinal cord injury causes chronic bone marrow failure. *Nature communications*. 2020 Jul 24;11(1):1-3.
69. Méndez-Ferrer S, Lucas D, Battista M, Frenette PS. Haematopoietic stem cell release is regulated by circadian oscillations. *Nature*. 2008 Mar;452(7186):442-7.
70. Sullivan J, Mirbahai L, Lord JM. Major trauma and acceleration of the ageing process. *Ageing research reviews*. 2018 Dec 1;48:32-9.
71. Lunnyak VV, Amaro-Ortiz A, Gaur M. Mesenchymal stem cells secretory responses: senescence messaging secretome and immunomodulation perspective. *Frontiers in Genetics*. 2017 Dec 19;8:220.
72. Zhu J, Lu K, Zhang N, Zhao Y, Ma Q, Shen J, Lin Y, Xiang P, Tang Y, Hu X, Chen J. Myocardial reparative functions of exosomes from mesenchymal stem cells are enhanced by hypoxia treatment of the cells via transferring microRNA-210 in an nSMase2-dependent way. *Artificial cells, nanomedicine, and biotechnology*. 2018 Nov 17;46(8):1659-70.
73. Phan J, Kumar P, Hao D, Gao K, Farmer D, Wang A. Engineering mesenchymal stem cells to improve their exosome efficacy and yield for cell-free therapy. *Journal of extracellular vesicles*. 2018 Dec 1;7(1):1522236.
74. Aicher A, Rentsch M, Sasaki KI, Ellwart JW, Fändrich F, Siebert R, Cooke JP, Dimmeler S, Heeschen C. Nonbone marrow-derived circulating progenitor cells contribute to postnatal neovascularization following tissue ischemia. *Circulation research*. 2007 Mar 2;100(4):581-9.
75. Nation DA, Tan A, Dutt S, McIntosh EC, Yew B, Ho JK, Blanken AE, Jang JY, Rodgers KE, Gaubert A. Circulating progenitor cells correlate with memory, posterior cortical thickness, and hippocampal perfusion. *Journal of Alzheimer's Disease*. 2018 Jan 1;61(1):91-101.
76. Hajjar I, Goldstein FC, Waller EK, Moss LD, Quyyumi A. Circulating progenitor cells is linked to cognitive decline in healthy adults. *The American journal of the medical sciences*. 2016 Feb 1;351(2):147-52.
77. Patel RS, Li Q, Ghasemzadeh N, Eapen DJ, Moss LD, Janjua AU, Manocha P, Al Kassem H, Veledar E, Samady H, Taylor WR. Circulating CD34+ progenitor cells and risk of mortality in a population with coronary artery disease. *Circulation research*. 2015 Jan 16;116(2):289-97.
78. Rigato M, Avogaro A, Fadini GP. Levels of circulating progenitor cells, cardiovascular outcomes and death: a meta-analysis of prospective observational studies. *Circulation research*. 2016 Jun 10;118(12):1930-9.
79. Kondo T, Hayashi M, Takeshita K, Numaguchi Y, Kobayashi K, Iino S, Inden Y, Murohara T. Smoking cessation rapidly increases circulating progenitor cells in peripheral blood in chronic smokers. *Arteriosclerosis, thrombosis, and vascular biology*. 2004 Aug 1;24(8):1442-7.
80. Fadini GP, Schiavon M, Cantini M, Baesso I, Facco M, Miorin M, Tassinato M, Kreutzenberg SV, Avogaro A, Agostini C. Circulating progenitor cells are reduced in patients with severe lung disease. *Stem Cells*. 2006 Jul;24(7):1806-13.

81. Mandraffino G, Aragona CO, Basile G, Cairo V, Mamone F, Morace C, D'Ascola A, Alibrandi A, Gullo AL, Loddo S, Saitta A. CD34+ cell count predicts long lasting life in the oldest old. *Mechanisms of ageing and development*. 2017 Jun 1;164:139-45.
82. Zahran AM, Abdel-Rahim MH, Refaat A, Sayed M, Othman MM, Khalak LM, Hetta HF. Circulating hematopoietic stem cells, endothelial progenitor cells and cancer stem cells in hepatocellular carcinoma patients: contribution to diagnosis and prognosis. *Acta Oncologica*. 2020 Jan 2;59(1):33-9.
83. Montaser LM, Sonbol AA, EL-Gammal AS, El-Yazeed AS. Role of circulating endothelial progenitor cells in patients with breast cancer. *Menoufia Medical Journal*. 2019 Jul 1;32(3):770.
84. Pedersen JK, Rosholm JU, Ewertz M, Engholm G, Lindahl-Jacobsen R, Christensen K. Declining cancer incidence at the oldest ages: Hallmark of aging or lower diagnostic activity?. *Journal of geriatric oncology*. 2019 Sep 1;10(5):792-8.
85. Pavlidis N, Stanta G, Audisio RA. Cancer prevalence and mortality in centenarians: a systematic review. *Critical reviews in oncology/hematology*. 2012 Jul 1;83(1):145-52.
86. Koh SH, Choi SH, Jeong JH, Jang JW, Park KW, Kim EJ, Kim HJ, Hong JY, Yoon SJ, Yoon B, Kang JH. Telomere shortening reflecting physical aging is associated with cognitive decline and dementia conversion in mild cognitive impairment due to Alzheimer's disease. *Aging (Albany NY)*. 2020 Mar 15;12(5):4407.
87. Cisterna BA, Vargas AA, Puebla C, Fernández P, Escamilla R, Lagos CF, Matus MF, Vilos C, Cea LA, Barnafi E, Gaete H. Active acetylcholine receptors prevent the atrophy of skeletal muscles and favor reinnervation. *Nature communications*. 2020 Feb 26;11(1):1-3.
88. Finger F, Ottens F, Springhorn A, Drexel T, Proksch L, Metz S, Cochella L, Hoppe T. Olfaction regulates organismal proteostasis and longevity via microRNA-dependent signalling. *Nature metabolism*. 2019 Mar;1(3):350-9.
89. Ruby JG, Smith M, Buffenstein R. Naked mole-rat mortality rates defy Gompertzian laws by not increasing with age. *elife*. 2018 Jan 24;7:e31157.
90. Miyawaki S, Kawamura Y, Oiwa Y, Shimizu A, Hachiya T, Bono H, Koya I, Okada Y, Kimura T, Tsuchiya Y, Suzuki S. Tumour resistance in induced pluripotent stem cells derived from naked mole-rats. *Nature communications*. 2016 May 10;7(1):1-9.
91. Hadi F, Kulaberoglu Y, Lazarus KA, Bach K, Ugur R, Beattie P, Smith ES, Khaled WT. Transformation of naked mole-rat cells. *Nature*. 2020 Jul;583(7814):E1-7.
92. Zhao Y, Tyshkovskiy A, Muñoz-Espín D, Tian X, Serrano M, De Magalhaes JP, Nevo E, Gladyshev VN, Seluanov A, Gorbunova V. Naked mole rats can undergo developmental, oncogene-induced and DNA damage-induced cellular senescence. *Proceedings of the National Academy of Sciences*. 2018 Feb 20;115(8):1801-6.
93. Wei H, Zhou W, Hu G, Shi C. Induction of mesenchymal stem cell-like transformation in rat primary glial cells using hypoxia, mild hypothermia and growth factors. *Molecular Medicine Reports*. 2020 Dec 10;23(2):1-
94. Tolstun DA, Knyazer A, Tushynska TV, Dubiley TA, Bezrukov VV, Fraifeld VE, Muradian KK. Metabolic remodelling of mice by hypoxic-hypercapnic environment: imitating the naked mole-rat. *Biogerontology*. 2020 Apr;21(2):143-53.
95. Place NJ, Prado AM, Faykoo-Martinez M, Brieño-Enriquez MA, Albertini DF, Holmes MM. Germ cell nests in adult ovaries and an unusually large ovarian reserve in the naked mole-rat. *R*
96. Leonida SR, Bennett NC, Leitch AR, Faulkes CG. Patterns of telomere length with age in African mole-rats: New insights from quantitative fluorescence in situ hybridisation (qFISH). *PeerJ*. 2020 Dec 4;8:e10498. eproduction. 2020 Nov 1;1(aop).
97. Gorbunova V, Bozzella MJ, Seluanov A. Rodents for comparative aging studies: from mice to beavers. *Age*. 2008 Sep 1;30(2-3):111.
98. Orr ME, Garbarino VR, Salinas A, Buffenstein R. Extended postnatal brain development in the longest-lived rodent: prolonged maintenance of neotenus traits in the naked mole-rat brain. *Frontiers in neuroscience*. 2016 Nov 8;10:504.
99. Penz OK, Fuzik J, Kurek AB, Romanov R, Larson J, Park TJ, Harkany T, Keimpema E. Protracted brain development in a rodent model of extreme longevity. *Scientific reports*. 2015 Jun 29;5:11592.
100. Zubieta-Calleja GR, Zubieta-DeUrioste NA. Extended longevity at high altitude: Benefits of exposure to chronic hypoxia. *BLDE University Journal of Health Sciences*. 2017 Jul 1;2(2):80.
101. Hachmo Y, Hadanny A, Hamed RA, Daniel-Kotovsky M, Catalogna M, Fishlev G, Lang E, Polak N, Doenyas K, Friedman M, Zemel Y. Hyperbaric oxygen therapy increases telomere length and decreases immunosenescence in isolated blood cells: a prospective trial. *Aging*. 2020 Nov 18;12.
102. Stindl R. The paradox of longer sperm telomeres in older men's testes: a birth-cohort effect caused by transgenerational telomere erosion in the female germline. *Molecular Cytogenetics*. 2016 Dec 1;9(1):12. <https://www.icpsr.umich.edu/web/pages/ICPSR/index.html>
103. Rencher, Alvin C.; Christensen, William F. (2012), "Chapter 10, Multivariate regression – Section 10.1, Introduction", *Methods of Multivariate Analysis, Wiley Series in Probability and Statistics*, 709 (3rd ed.), John Wiley & Sons, p. 19, ISBN 9781118391679. <https://www.ablebits.com/office-addins>

# Figures

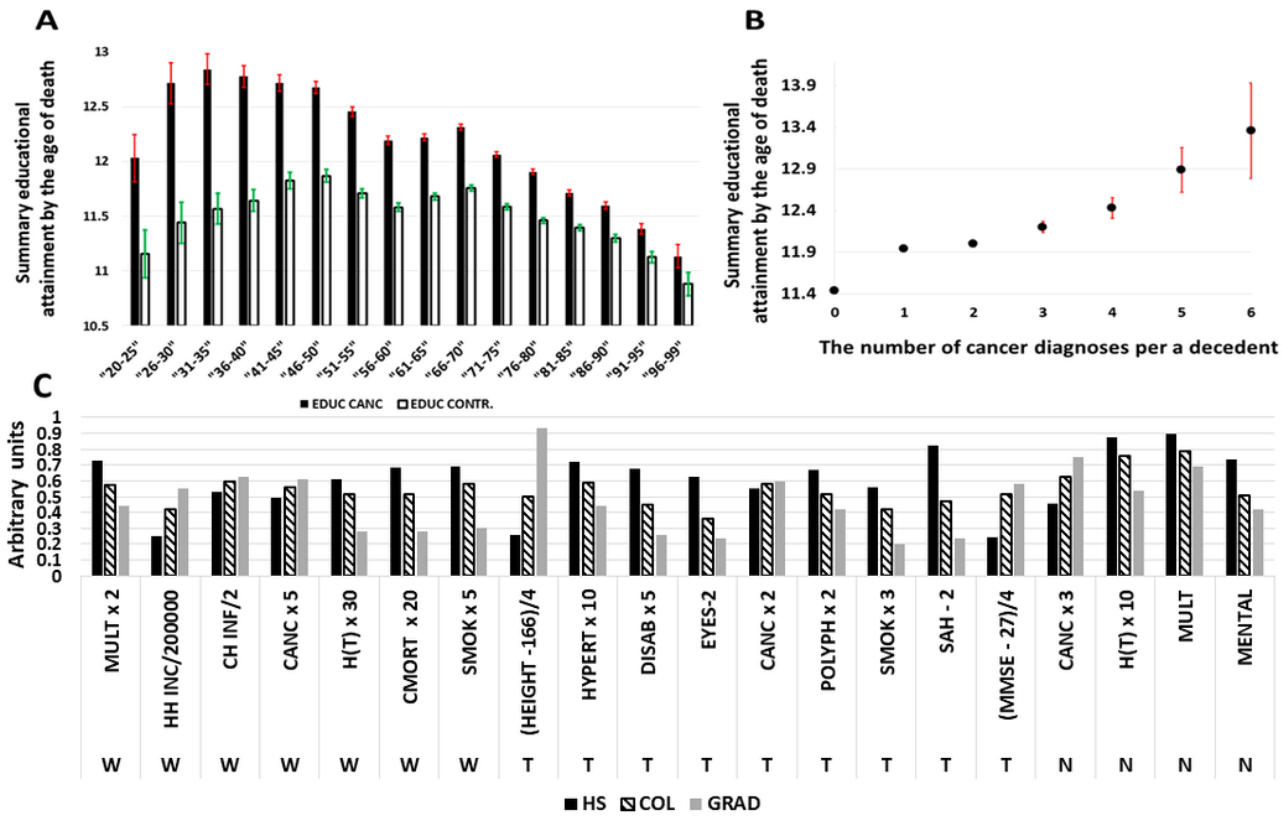


**Figure 1**

(A) Dependence of life-long educational performance on the cancer status and lifespan of the decedents. Plotted are the summary data for the 606228 cancer patient decedents (neoplasia as the primary diagnosis) and 1604462 non-cancer/non-dementia controls. The data were collected for the years 1999, 2004, 2011 and 2017 in the National Bureau of Economic Research (NBER), Multiple Causes of Mortality datasets. The abscissa represents 5-year brackets of lifespans. The average educational achievement by the educ1989 coding was plotted as a function of the achieved lifespan and neoplasia status. The random numbers were processed by the same procedure as education scores and provided the CI95 confidence intervals labeled in red and green. The educ1989 codes are: 0 - no formal education, 1-8 – years of the elementary and middle school, 9 – one year of high school, 10-two years of high school, 11 – three years of high school, 12- four years of high school, 13 – one year of college, 14- two years of college, 15 – three years of college, 16 -four years of college, 17 – five or more years of college. (B) Dependence of life-long educational performance on the number of cancer foci in the decedent. Plotted are the summary data for the 389589 cancer decedents (neoplasia as the primary diagnosis) and 1171054 non-cancer/non-dementia controls. The data were collected for the years 1999, 2004, 2011 and 2017 in the National Bureau of Economic Research (NBER), Multiple Causes of Mortality datasets. The ages were controlled in each foci number group and were equalized at 78 ( $\pm$  0.5) years in each stratum formed by the number of the foci per a person. (C) Reproducibility of the NBER data in Wisconsin Longitudinal Study (W, USA, N = 6385, average age 64.5), The Irish Longitudinal Study on Ageing (TILDA), 2013-2014 (T, Ireland, N = 5605, average age 65.5), National Health Interview Survey Series, 1994-2000, dataset 03807-0001 in ICPSR depository (N, USA, N =7131, average age 74 years). Each dataset was stratified based on education (black bars – elementary, middle, and high school or HS, striped bars – college or COL, grey bars – graduate or professional school or GRAD). In each stratum, different parameters were brought to the same scale. The parameters are: MULT – multimorbidity, measured as sum of cardiovascular disease, stroke, diabetes and renal disease in W, cardiovascular, stroke, diabetes, and respiratory disease in T and N; HH INC – household income; CH INF – childhood infections, including tonsillectomies; CANC – cancer; H(T) – annual probability of mortality, CMORT – cancer-associated mortality; SMOK -smoking rate; HEIGHT – height of a person; HYPERT – hypertension; DISAB- disabilities; EYES – residual vision acuity (1 = maximal acuity, 5 = minimal acuity); POLYPH – polypharmacy; SAH – self-assessed health (1 = best; 5 = worst); MMSE – mini-mental state examination; MENTAL – mental problems.

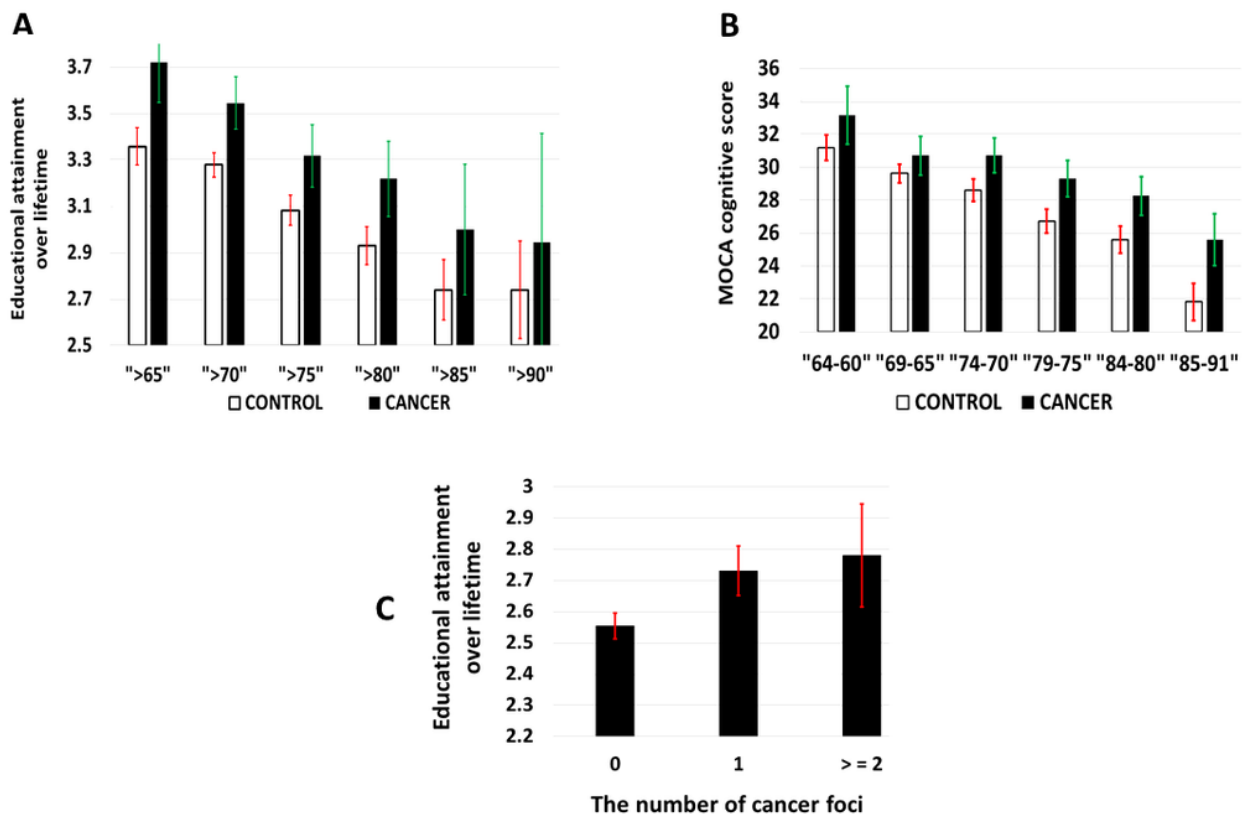


**Figure 2**

Dependence of academic performance and cognitive scores on the presence of cancer diagnosis as compared to the dementia-free control. A. Dependence of life-long educational performance as a function of age and neoplasia in NHIS 1994-2000 respondents, comparing cancer (N = 1721 respondents) and dementia-free control (N = 7575 respondents). Abscissa represents the 5-year ranges by age. The education levels are 0 – no formal education, 1- elementary school, 2-middle school, 3-high school, 4- college or university, 5 – graduate or professional school. B. Dependence of MOCA cognitive scores as a function of age and neoplasia in NSHAP 2005-2011 respondents, comparing cancer (820 respondents) and control (2400 respondents). Abscissa represents the 5-year ranges by age. C. Life-long educational performance in the individuals of the same age (73 years) with a variable number of cancer foci measured in NSHAP.

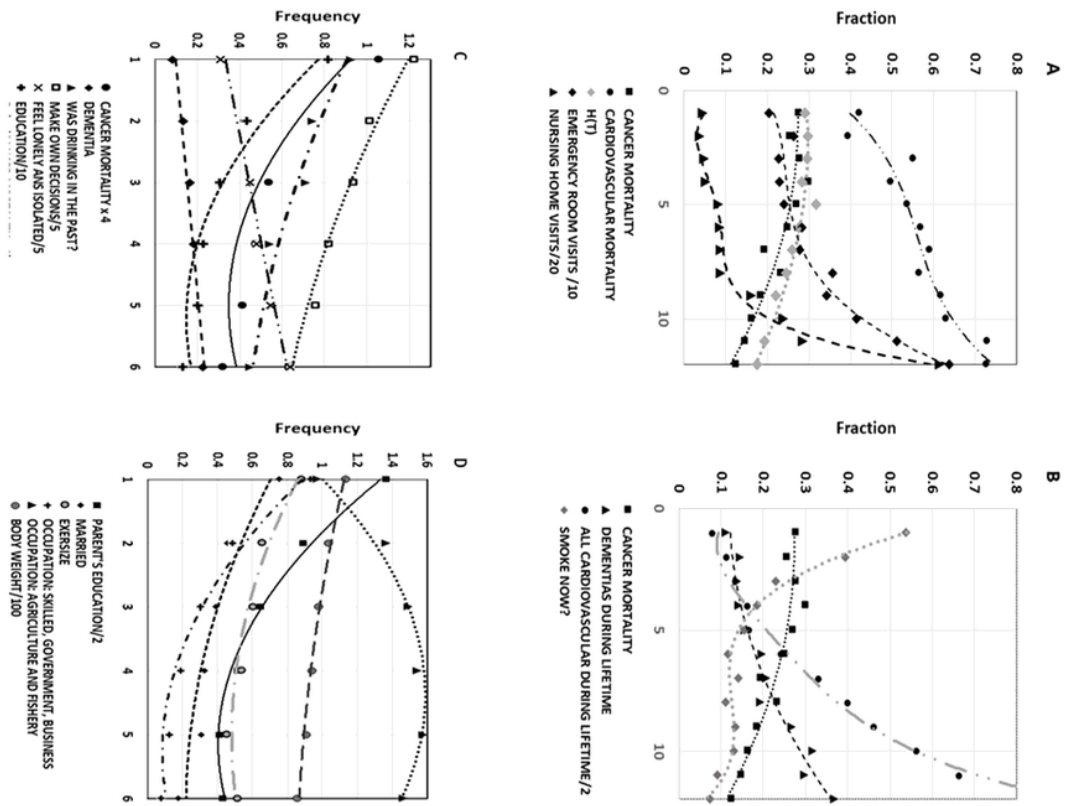


**Figure 3**

Validation of WLS results in the Kaiser Permanente Study of the Oldest Old (3A, 3B) and the Chinese Longitudinal Healthy Longevity Survey (CLHLS) (3C-D). A. Cancer mortality (ICD-9 codes) as a function of the multivariate regression predictor computed among 3200 decedents in the Kaiser Permanente Study of the Oldest Old, traced during a 8-year follow up at the baseline ages 75-90 years. The presence of lifestyle features and other comorbidities at the baseline correlates with the primary cause of death. The ranked population was divided in 12 percentile intervals on the abscissa in Figures 3A and 3B. The interval 1 is the most enriched in cancer mortality cases. The factors anti-correlating with the terminal neoplasia diagnoses are the emergency room visits per year (black rhombic symbols) cardiovascular mortality (black ovals) and nursing home visits per year (black triangular symbols), while all-cause mortality (H(T), grey diamonds) closely followed the cancer-specific mortality. The predicting features were measured at the baseline in the living patients, separated from the outcome by 7-8 years. The terminal cardiovascular disease diagnoses (black circles, dashed fitting line), the probability of dying in the current year H(T) (grey diamond symbols) represent the outcomes also predictable by the same set of factors. Thus, future cancer mortality correlated with decreased disability during follow up as compared to the comparable alternatives. B. Continuation of 3A. The factors correlating with cancer mortality fraction and other outcomes are smoking (grey rhombic symbols), while cardiovascular disease in the living patients (black circular symbols) and dementia in the living patients (black triangular symbols) are anti-correlating. The diagnoses in the living patients were collected at the baseline. C. Comparative distribution of predictive features and cancer presence in the 3872 decedents traced during the 3 year follow up in the Chinese Longitudinal Healthy Longevity Survey (CLHLS). The predictor rank produced as previously described is divided into 12 percentile intervals plotted on the abscissa. The graph presents cancer mortality (black circle symbols, solid fitting line), dementia presence (diamond symbols, simple dashed straight fitting line), alcohol abuse in the past (triangle symbols, dashed and dots fitting line), independent decision-making (empty square symbols), feeling lonely and isolated (cross-shaped symbols), education (vertical cross symbols). Educational achievement, independent decision-making and alcohol abuse in the past closely follow cancer mortality, while feeling lonely and isolated as well as dementia counter-correlate with cancer mortality. The individuals with less disfunction show greater propensity to cancer-related mortality in CLHLS. D. Continuation of 3C. The predictive features are plotted as a function of rank percentile: education of parents (square symbols, solid fitted line), married status (diamond symbols, short dashed fitted line), exercise (empty circle symbols, grey dashed fitting line), skilled labor, government, and business occupations (vertical cross symbols, short dash and dot fitted line), agriculture, horticulture and fishery occupations (triangle symbols), body weight (grey semi-empty circle symbols). The same model ranks the cancer mortality outcomes as already shown in 3C. The parent's education, married status, physical exercise and fitness, occupation in government, management, and skilled trades as well as absolute body weight correlate with cancer mortality, while the occupation in agriculture and

fishery are counter-correlates. Again, higher social status and intellectual/executive occupations favor cancer mortality outcomes vs. the comparative alternatives.

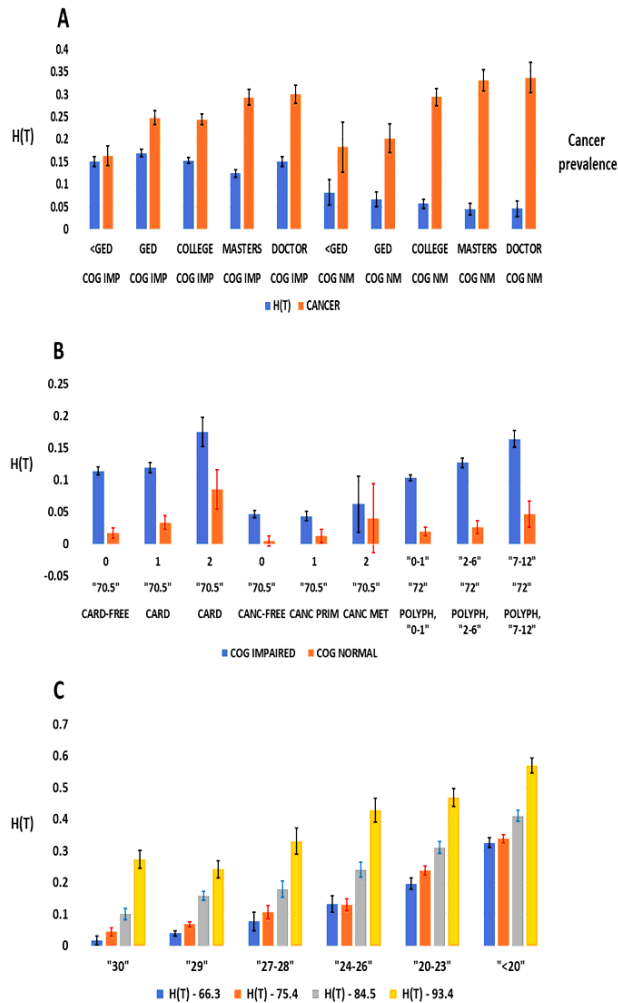


**Figure 4**

4A: The annual probability of mortality  $H(T)$  and cancer prevalence in the cognitively impaired patients ( $N = 17144$ , COG IMP; includes mild cognitive impairment and dementias during at least one visit) and in the patients cognitively normal during all visits ( $N = 5805$ , COG NM). Each sub-set is stratified by the lifetime academic achievement: incomplete GED (<GED), GED only, college, master's degree, doctorate, and professional school. The average age at baseline in each cohort is 78 years.  $H(T)$  was computed as the number of decedents accumulated in each cohort after the baseline and related to the length of follow up in each individual case. The individuals with the follow-up lengths < 1 year were excluded from the analysis. Cancer prevalence was measured by the presence of cancer in the patient at any time during the follow up, not only at the baseline. Figure 4B: The annual probability of mortality  $H(T)$  as a function of cognitive status and health. The  $H(T)$  values were computed as in (A). The cognitive status is defined as impaired (MCI or dementia, COG IMPAIRED,  $N = 15328$ ) or as normal (COG NORMAL,  $N = 7190$ ). The health status is defined as: no cardiovascular disease (CARD-FREE), a single cardiovascular disease, a combination of two cardiovascular conditions, no cancer, a single cancer locus (CANC PRIM), multiple cancer loci (CANC MET), polypharmacy 0-1, polypharmacy 2-6, polypharmacy 7-12 agents. The baseline ages of 70.5 and 72 years are indicated for the respective cohorts. Cancer data were computed in the version 3 of NACC, while the data for cardiovascular disease and polypharmacy are computed in the versions 1-3. Figure 4C: The annual probability of mortality  $H(T)$  as a function of cognitive status and age, the  $H(T)$  values computed as in (A). The population was stratified into the age of 66.3 years ( $N = 6672$ ), the age 75.4 ( $N = 8463$ ), the age 84.5 ( $N = 4209$ ), the age 93.4 ( $N = 425$ ), and these age cohorts were re-stratified by cognitive scores in the ranges: "30", "29", "27-28", "24-26", "20-23", "<20". For each cognitive score group, the ages were identified by the colors. In each bin of cognitive score, the ages follow the ascending order from left to right.

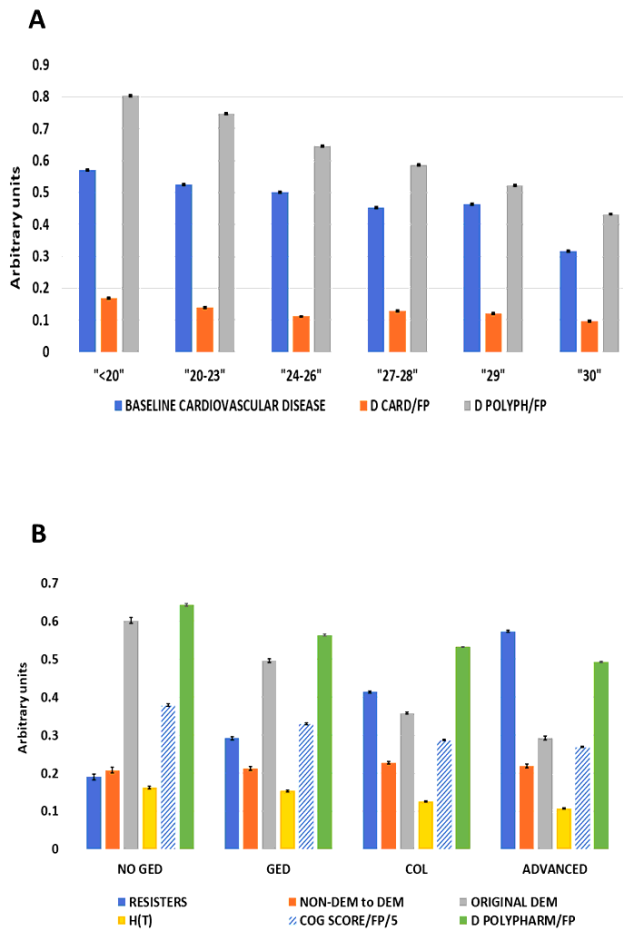


**Figure 5**

Measuring the rate of changes in the aging markers as a function of academic performance (a) and cognitive score (b) in NACC. a) The N = 17823 individuals at the baseline age 81 years were stratified by the educational performance in early life. The educational strata included the strata "no GED" (N = 1556, did not finish high school), "GED" (N = 3734, finished only high school), "COL" (N = 8429, college degree), "ADVANCED" (N = 4104, master's degree and doctorate, as well as the professional school equivalents). The 6 measurements in each category included the fraction of "resisters" (the patients cognitively normal at the baseline and the end of follow up, according to a clinician, resisting dementia conversion), "non-dem to dem" (the patients with normal cognitive status or with mild cognitive impairment at the baseline converting to dementia status), "dementia fraction at baseline" (dementia diagnosis at the baseline), H(T) (annual probability of mortality), COG SCORE/FP (the difference in the cognitive score over the follow up related to the length of follow up), D POLYPHARM/FP (the difference in the polypharmacy at the end of follow up and baseline related to the length of follow up). Variation was identified in a random model and adjusted to the size of the cohorts. b) The cognitive score strata (N = 14309) included the levels "30" (N = 3106), "29" (N = 1833), "27-28" (N = 2544), "24-26" (N = 2471), "21-23" (N = 1999), "<20" (N = 2536). For each level, the following metrics were computed: cardiovascular disease at baseline, the change in the fraction of cardiovascular disease related to the length of follow up, the change in polypharmacy level related to the length of follow up.

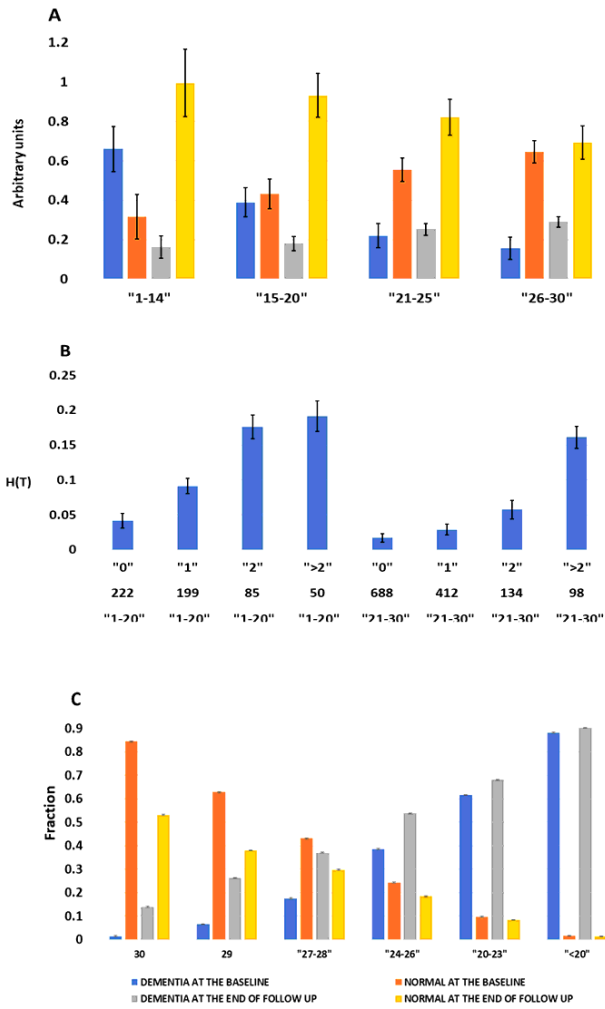


**Figure 6**

A. Reproducibility of the trends in Figures 4 and 5 produced in NACC in an independent dataset NSHAP (N = 2000, 68 years age at baseline). The bins "1-14", "15-20", "21-25", "26-30" refer to the components of MOCA cognitive score. In each bin, the leftmost blue bar refers to  $H(T) \times 5$ , the next orange bar is education code  $\times 0.2$  (1 – no GED, 2 – GED, 3- college, 4 – advanced degrees), the next grey bar is cancer prevalence fraction, the rightmost yellow bar in each MOCA bin is the multimorbidity (disease/person). B. Reproducibility of the trends in Figures 4 and 5 produced in NACC in an independent dataset NSHAP (N = 2000, 68 years age at baseline). The annual probability of mortality  $H(T)$  is a function of cognitive score range and the number of serious health conditions, measured as "0", "1", "2", ">2". The health conditions include any of heart attack, congestive heart failure, stroke, diabetes, osteoporosis, broken hip. The second row on abscissa indicates the number N of the patients in each cohort. The bottom row on the abscissa indicates the range of MOCA score as "0-20" and "21-30". C. Distribution of dementia and cognitive norm at the beginning and end of follow up (N = 23216, age 78 years at the baseline) in NACC. The cognitive score strata are shown along the abscissa.

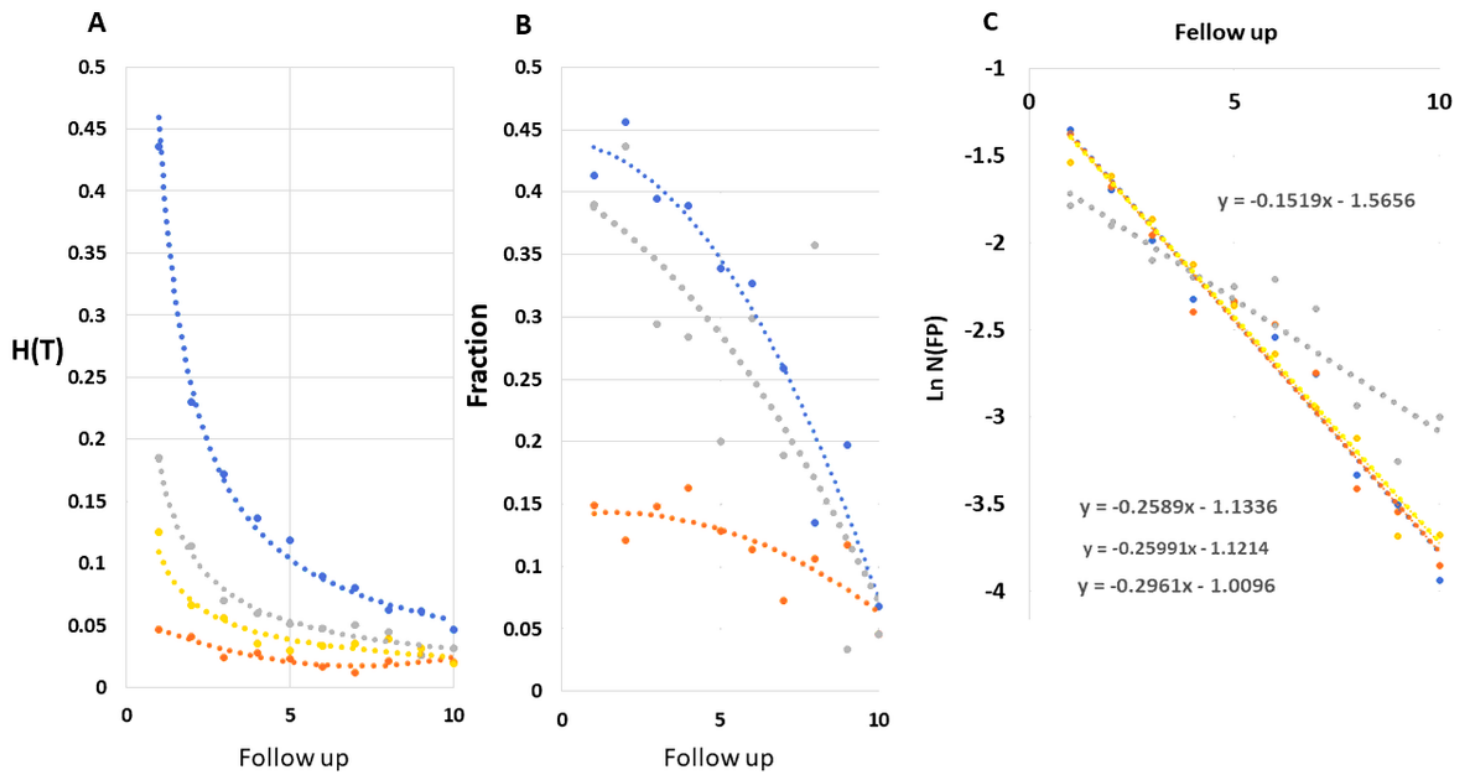
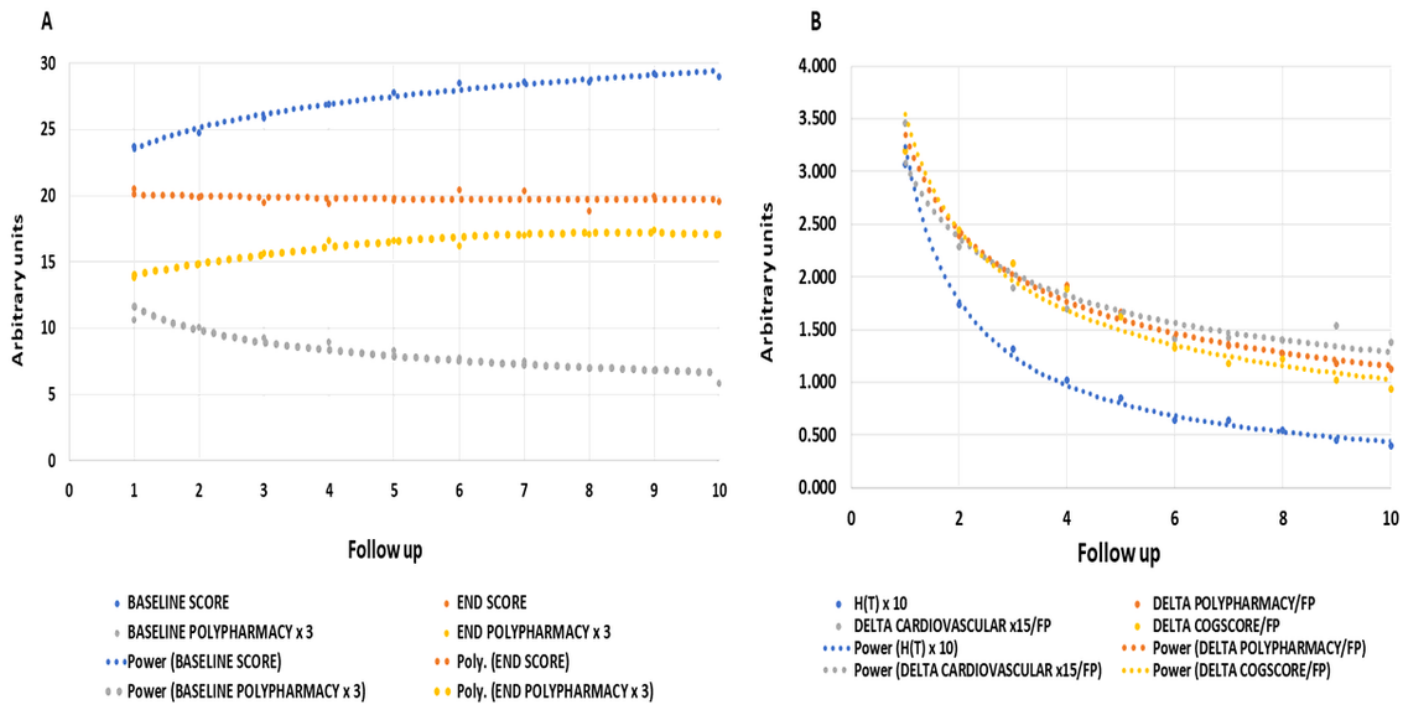


Figure 7

Comparison of low-score dementia converters, (+/+) high cognitive score dementia conversion resistors and (+/-) low cognitive score dementia conversion resistors, measured in  $N = 10417$  patients at the baseline of 79 years, the patients with the follow up 0 or with undefined cognitive scoring were excluded. A: Dependence of annual mortality probability  $H(T)$  on the length of follow up post-baseline in different phenotypes, plotted from top to bottom for dementia converters ( $N = 6633$ , blue line), high-score resistors ( $N = 1699$ , grey line), high score resistors with excluded cardiovascular morbidity subset ( $N = 1202$ , yellow line), and low-score resistors ( $N = 883$ , orange line). B: Dependence of the frequency of cardiovascular disease at the baseline in the patients of different dementia converter and resistors phenotypes. The top line refers to the dementia converters, followed by high-score resistors, followed by low-score resistors. C: Dependence of the attrition fractions of the respective populations on the length of follow up post-baseline. The annual fractions of attrition are plotted in logarithmic form  $\ln N(FP)$ , where  $N(FP)$  is the fraction of the patients leaving the study at the given follow up duration. The grey line apart from the rest refers to the low-score resistors (phenotype +/-), the closely clustered blue, yellow and orange lines refer to the dementia converters, high-score resistors, and high score resistors with the excluded cardiovascular disease subset.



**Figure 8**

Mortality surrogates and the annual mortality  $H(T)$  in the patient cohorts leaving the study at the different follow up intervals from the baseline ( $N = 10590$ , 80 years). A: The upper curve (blue) relates to the cognitive score at the baseline and the line below (orange) is the cognitive score at the end of follow up. The next (yellow) curve is the polypharmacy at the end of follow up brought to the scale (x3), the bottom (grey) curve is the polypharmacy at the beginning of follow up. B: The time-derivatives of cognitive score, cardiovascular disease, and polypharmacy as well as annual probability of mortality  $H(T)$  as functions of follow up length since the baseline. The derivatives are computed by relating the difference between the values at the end and beginning of follow up to the length of observation.

## Supplementary Files

This is a list of supplementary files associated with this preprint. Click to download.

- [Tableofsupportingfiles.docx](#)